



Contents lists available at ScienceDirect

## Computer Communications

journal homepage: [www.elsevier.com/locate/comcom](http://www.elsevier.com/locate/comcom)

## Content centric routing in IoT networks and its integration in RPL

Yichao Jin<sup>a,\*</sup>, Sedat Gormus<sup>b,1</sup>, Parag Kulkarni<sup>a</sup>, Mahesh Sooriyabandara<sup>a</sup><sup>a</sup> Toshiba Telecommunications Research Laboratory, 32 Queen Square, Bristol BS1 4ND, United Kingdom<sup>b</sup> Karadeniz Technical University, Trabzon, Turkey

## ARTICLE INFO

Article history:  
 Available online xxx

Keywords:  
 IoT  
 Routing  
 Content centric  
 Data aggregation  
 Implementation

## ABSTRACT

Internet of Things (IoT) networks can be used for many applications across different industry domains including infrastructure monitoring, civil service, security and surveillance applications etc. However, gathering large amounts of data from such networks including images and videos often cause traffic congestion in the central network area. In order to solve this problem, we proposed the content centric routing (CCR) technology, where routing paths are determined by content. By routing the correlated data to intermediate relay nodes for processing, a higher data aggregation ratio can be obtained, hence effectively reducing the traffic in the network. As a result, significant latency reduction can be achieved. Moreover, redundant data transmissions can also be eliminated after data aggregation which reduces the energy consumption spent predominantly on wireless communication thereby conserving limited battery. CCR was further integrated with the IETF RPL protocol and implemented in Contiki OS using the TelosB platform. Finally, both simulation and implementation results prove the superior performance of CCR in terms of low network latency, high energy efficiency, and high reliability.

© 2016 Published by Elsevier B.V.

## 1. Introduction

Distributed computing in wireless networks has recently been attracting a lot of attention, especially in the emerging paradigm of the Internet of Things (IoT) communications where IoT devices are equipped with independent processing, communication, and storage capabilities [1]. The key idea is that rather than sending all raw data directly across an expensive (multi-hop) wireless network which is usually correlated with high energy consumption and time delays, a more cost-effective way is to first reduce the data volume locally via in-network processing and subsequently forward only the processed result. Therefore, we can save bandwidth and energy, reduce latency and extend the network life in resource constrained IoT network [2].

In many cases, data collected for the same application tends to be highly correlated [3] and therefore can be combined or jointly processed while forwarding to the sink. For example, fusing together multiple sensor readings related to the same physical event. Such data aggregation process can reduce the total amount of

messages to be sent over expensive wireless links, which has a significant impact on energy consumption as well as overall network efficiency. On the other hand, uncorrelated packets might not be simply aggregated from the processing point of view, e.g. it is not meaningful to calculate an average of a temperature and a humidity reading. Therefore, one critical issue in data aggregation is to determine an optimized information flow and communication topology in order to efficiently route the correlated data to the intended processing nodes in the network. Let's take the tunnel monitoring system as an example to give more insight. As shown in Fig. 1, a variety of sensor nodes and cameras are installed to monitor two key tunnel assessments: tunnel structure safety and traffic management, where a huge amount of real-time sensory data including images and video streams needs to be delivered to a remote control centre. Traditionally, the server first collects all the data via the same routing topology regardless of whether the data is used for tunnel safety or traffic management. This case is illustrated in Fig. 1(A). Take Node 1 for example, it sends both Tunnel safety data A and traffic data B to node 5 as they are treated as the same. Once all data reaches the destination, the final results are computed at the server side. However, this is very likely to create a 'hot-spot' problem, where heavy network traffic in the central area results in higher energy consumption on the neck nodes and is also prone to traffic congestion events. This is due to the fact that the neck nodes are geographically closer to the access point/server, thus they have to forward messages coming from the outer regions (Fig. 1(A)).

\* Corresponding author. Tel.: +44 1179060780.  
 E-mail addresses: [yichao.jin@toshiba-trel.com](mailto:yichao.jin@toshiba-trel.com), [yichao.jin@hotmail.com](mailto:yichao.jin@hotmail.com) (Y. Jin), [sedatgormus@ktu.edu.tr](mailto:sedatgormus@ktu.edu.tr) (S. Gormus), [parag.kulkarni@toshiba-trel.com](mailto:parag.kulkarni@toshiba-trel.com) (P. Kulkarni), [mahesh@toshiba-trel.com](mailto:mahesh@toshiba-trel.com) (M. Sooriyabandara).

<sup>1</sup> This work was carried out when the author was with Toshiba Research Europe Ltd.

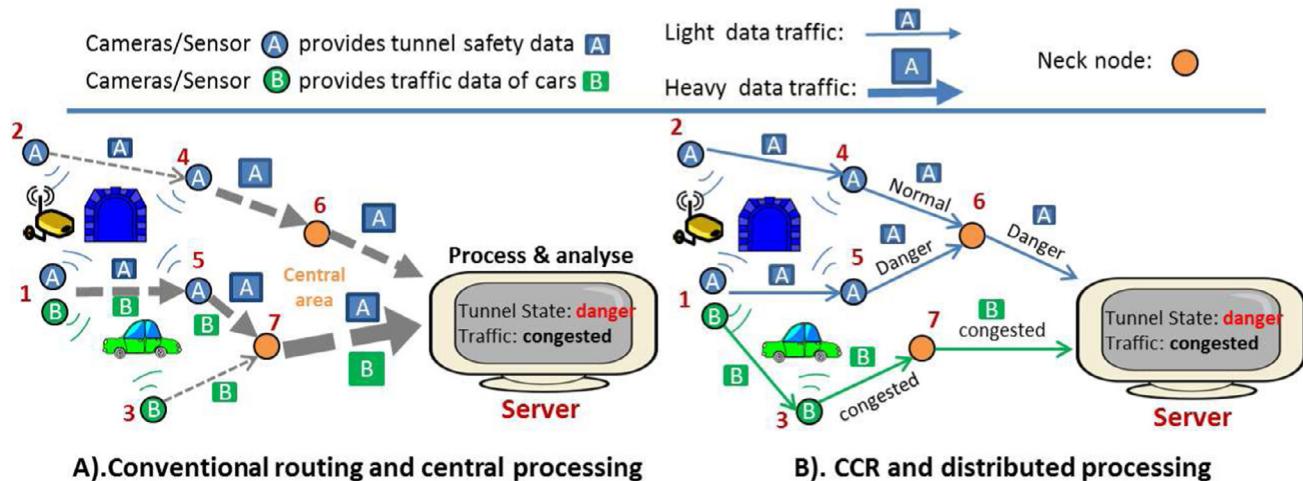


Fig. 1. Conventional routing vs. CCR.

To overcome such problem, we proposed a content centric routing (CCR) protocol in [4] for efficient data aggregation in multi-hop IoT networks. We differentiate data by its content while routing information, and correlated data are termed as the data of the same content. As shown in Fig. 1(B), since both Node 1 and Node 3 provide information for traffic conditions, rather than sending content B to Node 5 as shown in Fig. 1(A), Node 1 sends it to Node 3 where they can be combined or aggregated while forwarding to the server. Intermediate results such as heavy traffic warnings can be computed within the network. As a result, two distinctive routing topologies based on content A and B are created in CCR. This can help to reduce the amount of redundant data sent over the network and also the time lag in the communication system, saving limited node energy and extending the network lifetime.

CCR provides a paradigm shift from traditional ways of data collection to content oriented data aggregation and retrieval. This change could bring several attractive advantages such as energy efficiency, fast system response, long network lifetime etc. and provides a way to solve the data explosion problem [5] for the future IoT network. In [4], we proposed a multi-objective function to provide optimized in-network data aggregation with the aim of reducing latency, load balancing and extending the network lifetime. Using which, each node can refine its routing strategy according to neighboring traffic patterns and the energy availability of the neighboring nodes. In addition, a routing candidate selection mechanism was developed in order to avoid communication loops, and the signaling cost of local message gossiping is controlled to conserve limited node energy and resources. With respect to our previous work, in this paper, we further extend the analysis and protocol explanations in [4], including updated frameworks, signaling and control message details, and trigger function flows etc. Furthermore, we presented a possible integration of CCR in a real industrial standard (the IETF RPL protocol [6]). The implementation is based on the Contiki OS<sup>2</sup> and TelosB platform. Last but not least, CCR is evaluated by both simulation and implementation experiments. To the best of our knowledge, this paper is the first to present how to implement a content based routing protocol for in-network data aggregation.

The rest of the paper is organized as follows. Section 2 covers the related work. In Section 3, we present our models and assump-

tions following which we present the CCR protocol in Section 4. The CCR implementation and integration with RPL is illustrated in Section 5. The efficacy of the design is illustrated in Section 6 with both simulation and emulation results. The paper finally concludes in Section 7 highlighting some of the key findings.

## 2. Related work

Different from recent popular notion of Content-Centric Networking (CCN) or Named Data Networks (NDN) [8]–[10] which has a aim of caching and subscribing data based on content rather than the host. The main focus of the proposed CCR technology is to provide optimized routing topology to facilitate in-network data aggregation and reduce the network traffic.

Routing and data aggregation mechanisms have received considerable attention in the literature [3], [11] in the context of wireless sensor networks. The existing body of work can be broadly classified into two categories – centralized and distributed approaches. Centralized approaches [12]–[17] usually pre-compute and construct the optimal appropriate routing structure before the network starts to operate. In [13], a network lifetime maximum aggregation tree solution is proposed. Load balancing is considered in [15], and authors in [17] further took the aggregation computational cost into account. However, global network information is often required for above literatures which can introduce significant control overhead. In order to reduce control overhead, distributed clustering approaches such as [18]–[24] resort to forming hierarchical routing topologies via local message gossiping. However, only a simple shortest path tree topology is adopted in [22]. In [23], a dynamic clustering based approach is proposed. However, the clustering process is triggered per event or application, resulting in large transmission cost in forming the clusters. In addition, similar to the clustering approach, tree ([13], [14], [25]) or Direct Acyclic Graph (DAG)[26] based approaches also require a specific routing topology to operate, and hence limits their abilities to cope with dynamic network conditions. This is because each time a network change happens such as link breakage or early energy depletion of some critical routing nodes, the network topology information needs to be updated to reflect the prevailing conditions. This, however, has the cost of introducing additional control traffic to the network as well as incurs additional delays.

<sup>2</sup> Contiki is an operating system to network embedded devices. It is highly portable and can be ported to more than 12 different microprocessor and micro-controller architectures. [7]

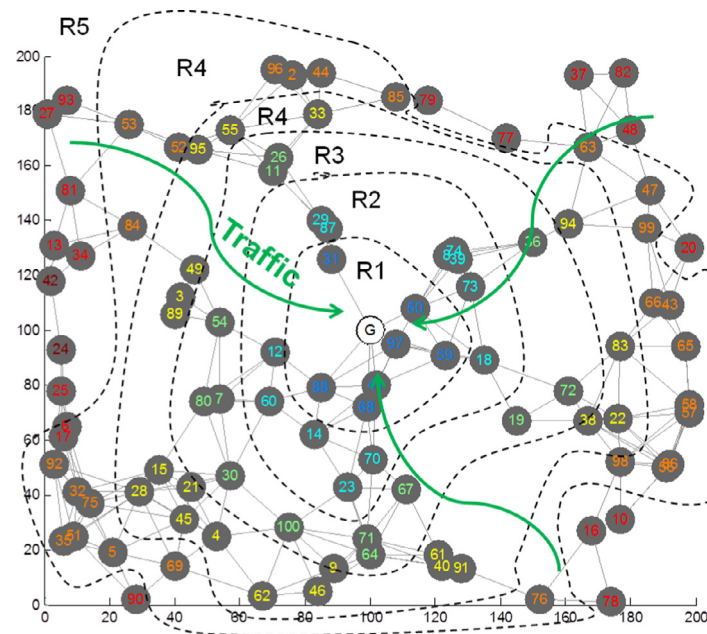


Fig. 2. Hop distance based ring topology [4].

127 A key shortcoming of existing solutions is that they often as-  
 128 sume homogeneous network conditions, for example: homogenous  
 129 traffic or universal node processing capability. However, traffic is  
 130 dynamic in nature. Each time the traffic of an application changes  
 131 or a new application arrives, the optimized network structure  
 132 should, ideally, also be re-formed. In a dynamic environment with  
 133 multiple applications co-existing, different data aggregation paths  
 134 are required for efficient delivery of different types of data and  
 135 better organization of heterogeneous traffic flows. A pre-optimized  
 136 static structure cannot satisfy the requirements in such a scenario.  
 137 On the other hand, it is not computationally efficient to frequently  
 138 reconstruct a global network topology or to compute and build  
 139 multiple overlaid topologies because such approach would be ex-  
 140 pensive to maintain in lossy environments.

141 On a related note, a perfect channel condition is also usually as-  
 142 sumed [4], [21], [27], which may not always be the case in the real  
 143 world as communication link quality can vary over time. Such an  
 144 assumption can jeopardize the delivery of a message and can po-  
 145 tentially result in re-transmissions which result in further energy  
 146 depletion. Routing packets based on link quality and connectivity  
 147 can improve communication reliability [6] but it does not necessar-  
 148 ily lead to energy efficient routing. Thus, in addition to improving  
 149 communication reliability, conserving the limited on-board energy  
 150 of the battery powered nodes is an important requirement in order  
 151 to keep the nodes alive and running in such resource constrained  
 152 networks.

153 To overcome some of the problems above, the CCR algorithm  
 154 [4] was introduced to provide content based information flow and  
 155 optimized in-network data aggregation with the aim of avoiding  
 156 the transmission of redundant network traffic, reducing network  
 157 delay, conserving limited energy resource and extending the net-  
 158 work lifetime. Furthermore, compared with our previous work [4],  
 159 we provide analysis on a possible integration of CCR in a real  
 160 IoT protocol stack. CCR is modified such that it can be integrated  
 161 with the RPL protocol and show its compatibility with a stan-  
 162 dard based protocol stack. Its effectiveness is evaluated via both  
 163 Matlab simulation and more practical Contiki Cooja based emula-  
 164 tion. A small scale CCR implementation Demo based on real hard-  
 165 ware (TelosB mote) was developed and demonstrated on various  
 166 occasions.

### 167 3. System models and assumptions 168

#### 169 3.1. Network model 170

171 We assume that nodes send data to a gateway node residing at  
 172 the centre of the topology. The gateway node is much more capa-  
 173 ble (e.g. in terms of processing power, memory etc.) than the indi-  
 174 vidual nodes themselves and has access to mains power. Nodes are  
 175 battery powered and have a finite and heterogeneous initial energy  
 176 supply  $E(i)$ . Transmission power control is not enabled and there-  
 177 fore all nodes have a fixed communication range. We also assume  
 178 heterogeneous node processing capability, e.g., a node may only be  
 179 capable of processing one or a few particular types of content due  
 180 to hardware or software constraints. In case a node receives a data  
 181 packet that it cannot process, it simply relays the packet. To begin  
 182 with, the gateway broadcasts a radio ranging message to help the  
 183 nodes ascertain how many hops away are they located from the  
 184 gateway. Nodes that receive this message are assigned with a layer  
 185 ID. This layer ID represents the minimum hop distance between a  
 186 node and the gateway. Subsequent to assignment of the layer ID,  
 187 the node forwards this message with its own layer ID included in  
 this message. Such a wave like propagation, results in the forma-  
 tion of a ring type of topology as shown in Fig. 2.

#### 188 3.2. Application and aggregation mode

189 We mainly consider monitoring applications (multi-point to  
 190 point data collection scenario) in this paper for data aggregation  
 191 purpose. All data packets associated to the same processing ob-  
 192 jective are termed as the packet of the same content, which then  
 193 can be processed by a corresponding processing node. For exam-  
 194 ple, same type of data (temperature readings) gathered in a build-  
 195 ing can be treated as the same content if an application requires  
 196 the average building temperature. For simplicity, we assume that  
 197 each application running in the network only has a single pro-  
 198 cessing objective, but multiple applications can co-exist. A total  
 199 number of  $K$  applications  $A = \{a_k \mid k = 1, 2, 3, \dots\}$  have the same  
 200 poisson arrival rate of  $\lambda$ , but with different running duration of  
 201  $T = \{t_k \mid k = 1, 2, 3, \dots\}$  and heterogeneous traffic data rates  
 202  $R_k$ . Depending on the accuracy requirement of an application,

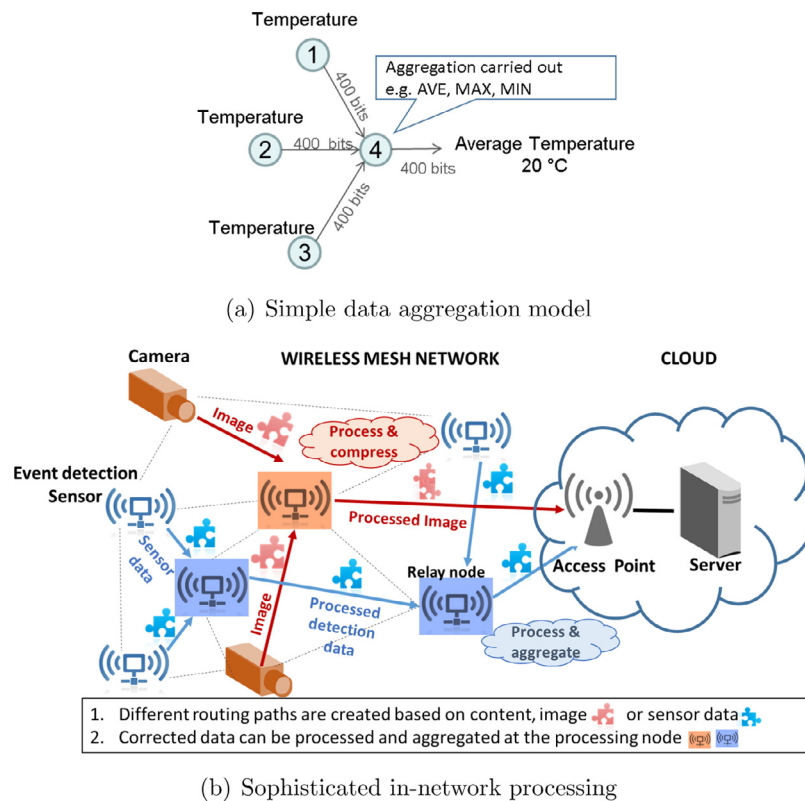


Fig. 3. Aggregation model examples for different applications.

203 different data aggregation functions can be applied considering  
 204 lossy or lossless aggregation processes [28]. For each node  $i$  with  
 205 processing function  $s$ , a generic data aggregation model is defined  
 206 below:

$$R_i^{out} = \omega_s \times R_i^{in} \quad (1)$$

$$0 < \omega_s \leq 1$$

207 where  $R_i^{in}$  and  $R_i^{out}$  represent the incoming and outgoing traffic  
 208 rate, respectively.  $\omega_s$  is the data aggregation or compression rate  
 209 depends on the processing function  $s$ . If  $\omega_s = 1$ , it means that the  
 210 current content cannot be processed by  $s$ .  $\omega_s$  can also be a variable  
 211 depending on the processing function. For example, there may be  
 212 considerable correlation of data streams comprising data reports of  
 213 AVERAGE or MAX readings for monitoring applications, which can  
 214 aggregate multiple incoming messages into a single outgoing mes-  
 215 sage. In such cases, depending on the total received message num-  
 216 ber (assuming  $M$ ) on an aggregation node,  $\omega_s$  could be  $\frac{1}{M}$ . Never-  
 217 theless, we assume only messages from the same application can  
 218 be aggregated. For reasons, different data types may not be easily  
 219 processed or just not possible to do so in some cases. For example,  
 220 it is not meaningful to calculate the average value of a tempera-  
 221 ture and a humidity reading. An example of data aggregation can  
 222 be found in Fig. 3.

223 In order to have a good data aggregation opportunity, it is assumed  
 224 that aggregation is carried out in a periodic manner at each hop,  
 225 i.e. each node waits for a pre-defined period of time to gather  
 226 information [29] and then performs the aggregation. A timeout  
 227 clock is used in case some packets get lost during transmission.

#### 228 4. The proposed CCR protocol

229 CCR is a distributed process, when an application arrives at the  
 230 gateway following which a default routing structure is first used  
 231 to initiate data collection. The focus of the subsequent phases is

232 about optimizing this routing structure. Each node has a probabil-  
 233 ity  $p_t$  to refine its next hop relay by executing an objective func-  
 234 tion  $F$ . The node that intends to execute  $F$  (referred to as an objective  
 235 node hereafter), first broadcasts a local query message to its one-  
 236 hop neighboring nodes. The query message comprises the objective  
 237 node's outgoing traffic content types and corresponding traffic vol-  
 238 ume, and the candidate selection criterion (TTGF bits described in  
 239 Section 4.3). The qualified next hop candidate will then respond to  
 240 it with an ACK message, which consists the information required  
 241 by  $F$  such as the responder's ID and the estimated node lifetime of  
 242 the responder if the designated traffic was sent to that candidate  
 243 node. Using this information as the input of the objective func-  
 244 tion, candidate rankings are produced and the one with the highest  
 245 ranking is selected to relay the corresponding traffic. Finally, the  
 246 objective node updates the routing table and broadcasts a route  
 247 update announcement message containing new next hop node ID  
 248 for corresponding traffic content. Subsequently, the new next hop  
 249 nodes reply with JOIN ACK messages and the previous relay nodes  
 250 send LEAVE ACK messages. As a result of this process, an overlaid  
 251 tree topology for multiple traffic content types can be updated dy-  
 252 namically. Details of the message sequence signaling involved in  
 253 this process is illustrated in Fig. 4.

254 CCR's operation includes three main functions: trigger function,  
 255 objective function, and routing updates with loop detection func-  
 256 tion, and its system architecture is shown in Fig. 5. The trigger  
 257 function decides how frequently to execute the CCR objective func-  
 258 tion. It ensures a high execution frequency under dynamic net-  
 259 work conditions in order to keep the routing table up-to-date, and  
 260 a low execution frequency when the network stabilizes to reduce  
 261 the cost of local signaling. Once the objective function is triggered,  
 262 the node queries its neighbors to provide some information such  
 263 as data traffic status, remaining battery power level and the con-  
 264 tent in their own routing tables. Using this information as the in-  
 265 put of the objective function, candidate rankings are produced and

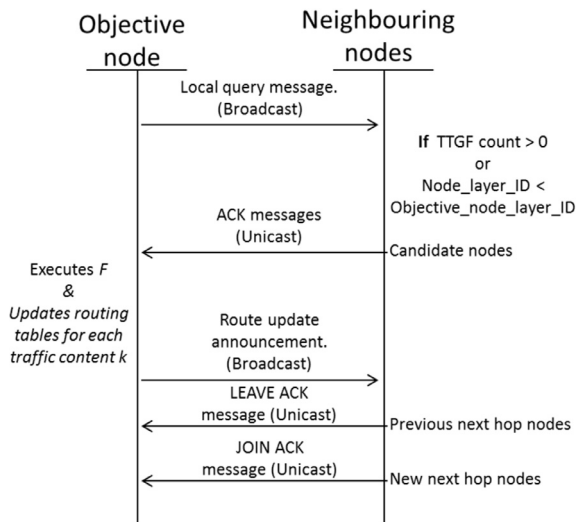


Fig. 4. CCR signaling messages.

the one with the highest ranking is selected to route the corresponding content. Hence, the objective function constructs a separate routing entry for each content in the routing table. Lastly, an effective loop avoidance mechanism is designed in order to detect communication loops and conserve the limited amount of energy stored at each node. Details of each function are described in the following sections.

#### 4.1. Trigger function

In dynamic network environments, most routing protocols periodically update their routing information and keep the routing table up to date. This, however, incurs additional control overheads. In resource constrained networks with lossy links, these signaling messages should be controlled in order to conserve limited on-board node energy.

The frequency of executing the objective function at a time  $t$  is controlled by a probability  $p_t$ . This probability is calculated independently on each node and does not require any local or global network information.  $p_t$  is defined as below:

$$p_t = \min \left( \left( \sum_{t_1}^t |\Delta_k| + 1 \right) \times p_{default}, 1 \right) \quad (2)$$

Where  $\Delta_k$  is the traffic content variation of each node at a time round.<sup>3</sup>  $t$  is the current time instance while  $t_1$  is the previous time instance when the node ran the objective function.  $p_{default}$  is the default probability determined by system parameters, details of this can found in Section 6.1.2. An example of variation of  $\Delta_k$  is shown in Fig. 6(a), and the system function flow to execute  $F$  based on  $p_t$  is illustrated in Fig. 6(b).

Thus, the probability of executing the objective function increases if a large value of  $\Delta_k$  is produced due to traffic content variation. On the other hand, when the network stabilizes (small  $\Delta_k$ ), the probability  $p_t$  decreases. It becomes  $p_{default}$  if no changes occur, which effectively reduces control overhead. This ensures that even in a slow changing environment, the routing table is still kept updated. Yet, the probability to execute the objective function is much lower in a stable network compared to a dynamically changing one.

#### 4.2. The objective function ( $F$ )

The objective function  $F$  is executed on an objective node  $i$  in order to find out the most suitable next hop node  $j$  for each traffic content  $k$  among  $N$  neighboring candidates. Since the traffic is differentiated by its content type, the objective node maintains a separate routing entry for each content  $k$  and updates it by executing the objective function. Details of the objective function are described as below in (3).

$$F(k) = \max_{j \in N} \left( \tilde{g}_j^k - g_j^k + \beta \frac{\tilde{l}_j^k - l_j^*}{\tilde{l}_j^k} + \varepsilon_j^k \right) \quad (3)$$

where the first term  $\tilde{g}_j^k - g_j^k$  calculates the normalized communication data reduction via aggregation process which is called as the marginal processing gain. The second term  $\frac{\tilde{l}_j^k - l_j^*}{\tilde{l}_j^k}$  is the link quality

aware local network lifetime gain estimation; while  $\beta$  is a tuning parameter to provide weights between the two parameters. Finally,  $\varepsilon_j^k$  is a reward parameter. We'll explain each parameter in the following sections.

##### 4.2.1. The processing gain

The first term in (3),  $\tilde{g}_j^k$  is the processing gain by allocating application content  $k$ 's traffic to Node  $j$ , and  $g_j^k$  is the processing gain without allocating content  $k$ 's traffic to  $j$ , where  $g_j^k$  is calculated as:

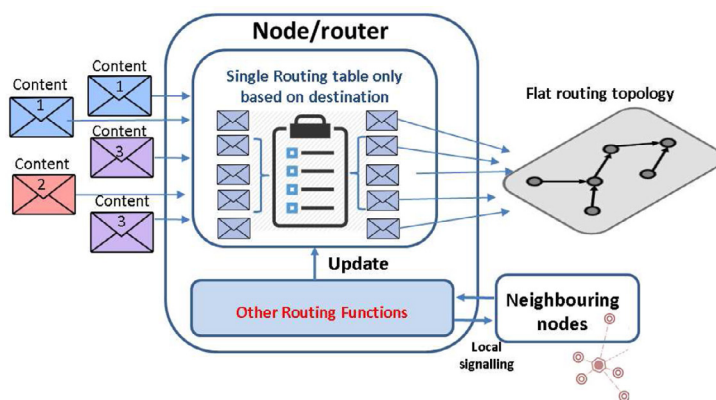
$$g_j^k = \frac{\sum_{k \in K} R_j^{in}(k) - \sum_{k \in K} R_j^{out}(k)}{\sum_{k \in K} R_j^{in}(k)} \quad (4)$$

Basically,  $\sum_{k \in K} R_j^{in}(k)$  and  $\sum_{k \in K} R_j^{out}(k)$  stand for the total amount of incoming and outgoing traffic for total  $K$  applications on Node  $j$ , respectively. Therefore, the numerator of (4) represents the total amount of traffic reduction via data aggregation at node  $j$ . This value is then divided by the total incoming traffic. The rationale behind this parameter is:

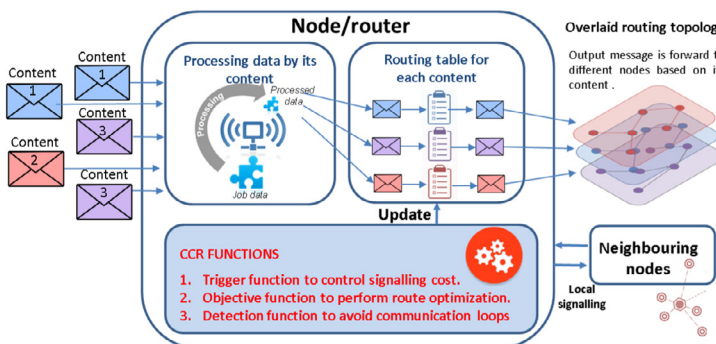
- It is the normalization process which makes the marginal processing gain numerically comparable with the local lifetime gain (second term shown in (3)) and therefore facilitates computation of a multi-gain and,
- For load balancing purposes, it is preferable to relay traffic to a node that can provide the same processing gain (reduce the same amount of data), but with less traffic than is already assigned to it. In other words, with the same amount of reduction in traffic achievable through aggregation, the more incoming traffic a node has, the smaller processing gain it can obtain.

An example illustrating the above concept is shown in Fig. 7. Two applications ( $a_1$  &  $a_2$ ) are collecting data in a network formed by 6 nodes. Nodes 1–3 are the source nodes of  $a_1$  and Node 4 is the source node for application  $a_2$ . It is assumed that both Nodes 4 and 5 can process  $a_1$  and  $a_2$  with  $\omega_{a_1} = \omega_{a_2} = 1/M$ .<sup>4</sup> Assume that Node 3 is executing the objective function to determine which of the two nodes (Node 4 or Node 5) should forward its traffic ( $a_1$ ). Clearly, in this example, Node 5 will be selected as it has a better processing gain due to the fact that it is only ferrying traffic for a single application type and therefore can aggregate information unlike Node 4 which cannot aggregate traffic as it is transporting data for two different types of application.

<sup>4</sup> Mis the total number of messages received for the same application as described in Section 3.2.

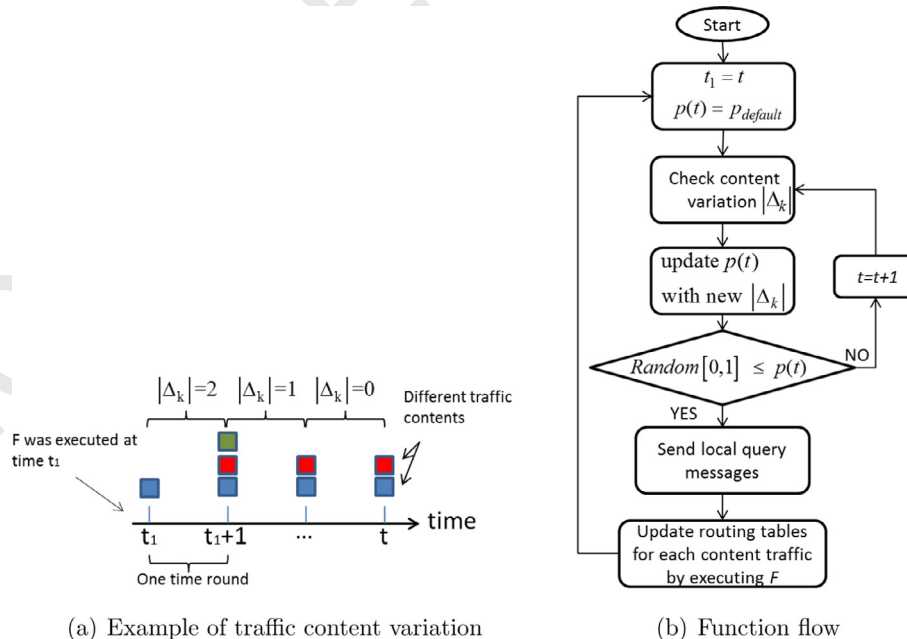


(a) Conventional approach with single routing topology



(b) CCR creates an overlaid routing topology based on content

Fig. 5. CCR architecture and operational difference.



(a) Example of traffic content variation

(b) Function flow

Fig. 6. Dynamic trigger function.

348 By taking advantage of the processing gain, the amount of communication traffic can be reduced by aggregating correlated data. 349 However, this does not necessarily imply that a longer network lifetime can be achieved because energy consumption could be 350 higher if the selected link has a very poor channel quality. Furthermore, heterogeneous node energy levels need to be considered as, in principle, if a node is equipped with more energy it can relay and process more information compared with those with 351 352 353 354 355

less on-board energy. Therefore, another parameter is introduced in the objective function shown in Eq. (3), known as the link quality aware local lifetime gain. 356 357 358

4.2.2. Link quality aware local lifetime estimation 359

Due to the inherent nature of the wireless medium, link quality can vary. There are various link quality estimation methods. For example, ETX (Expected Transmission count) [30] is a popular link 360 361 362

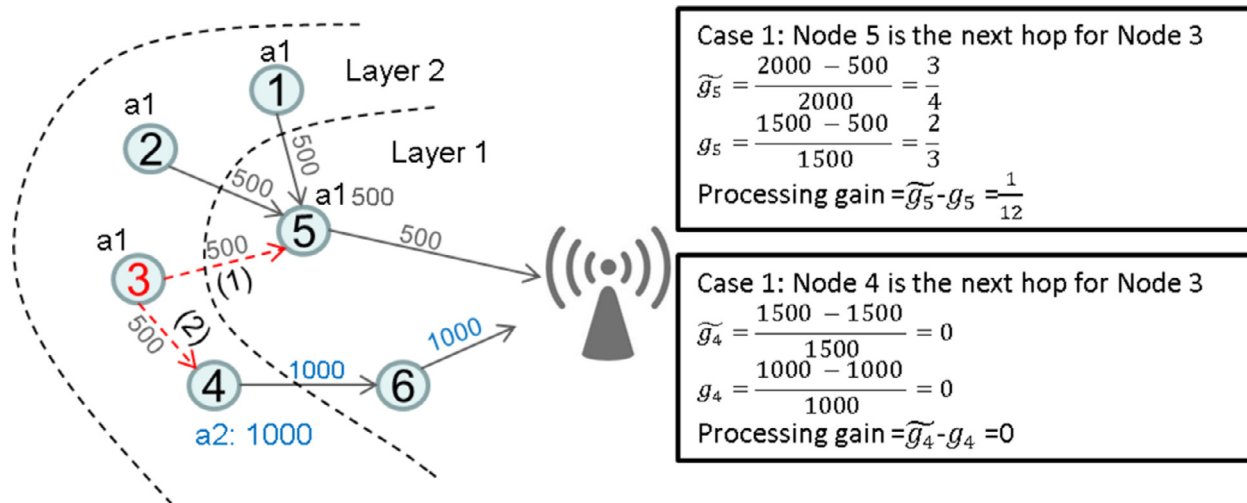


Fig. 7. Examples for processing gain.

363 quality/reliability parameter used in many routing protocols such  
 364 as RPL [6]. ETX is the average number of transmissions required by  
 365 a sender to successfully deliver a message to the destination.

366 Since the ETX value of a link can be easily converted to the  
 367 average amount of energy spent on transmissions per packet via  
 368 that link, we chose this parameter to assess the communication  
 369 link quality. This further contributes to estimation of the local net-  
 370 work lifetime. Even though ETX is used in this work, it should be  
 371 possible to use other link quality metrics with simple modification  
 372 to the estimation function.

373 The local lifetime gain parameter  $\frac{l_j^k - l_j^{*k}}{l_j^k}$  shown in (3) is defined  
 374 as the minimum node lifetime among the objective node  $i$  and its  
 375  $N$  qualified neighboring candidate nodes.

$$l = \min \left( \frac{E_i}{e_i}, \min_{j \in N} \left( \frac{E_j}{e_j} \right) \right) \quad (5)$$

376 where  $E_i$  and  $E_j$  is the current battery energy level for the objec-  
 377 tive node and the candidate node respectively; and  $e_i$  and  $e_j$  is the  
 378 total energy consumption including processing, transmission and  
 379 reception costs. In (3),  $l_j^{*k}$  stands for the current local network life-  
 380 time which can be simply obtained via the query process shown in  
 381 Fig. 4. While  $l_j^k$  is the estimated local network lifetime if the con-  
 382 tent  $k$ 's traffic is allocated to a new candidate  $j$  rather than  $j^*$ . In  
 383 order to calculate  $l_j^k$ , the estimated energy consumption of the ob-  
 384 jective node  $\tilde{e}_i$  and each candidate node  $\tilde{e}_j$  have to be estimated by  
 385 considering switching the content traffic  $k$  from the current next  
 386 hop node  $j^*$  to a new candidate node  $j$ . Thus, for each candidate  
 387 node  $j$  ( $j \neq j^*$ ),  $\tilde{e}_j^k$  can be calculated as:

$$\tilde{e}_i^k = e_i^* - (ETX_i^{j^*} - ETX_i^j) \times U^k \times e_t \quad (6)$$

388 where  $ETX_i^{j^*}$  and  $ETX_i^j$  stand for the ETX value of the current link  
 389 from  $i$  to  $j^*$  and the link from  $i$  to a candidate node  $j$  respectively,  
 390  $U^k$  is the total amount of data for traffic  $k$  and  $e_t$  is the average  
 391 energy consumption to transmit one bit of data.

392 Similarly, the estimated energy consumption  $\tilde{e}_j^k$  ( $j \neq j^*$ ) can be  
 393 obtained as shown in (7).

$$\tilde{e}_j^k = e_j^* + U^k \times e_r + U^k \times e_p + ETX_j^{NextHop} \times U_p^k \times e_t \quad (7)$$

394 where  $e_r$ ,  $e_p$  are the energy consumption to receive and process  
 395 one bit of data and,  $U_p^k$  is the amount of additional data after pro-  
 396 cessing which  $j$  has to send to its next hop node. If node  $j$  cannot  
 397 process content  $k$ , then  $U_p^k = U^k$ .

#### 4.2.3. Reward parameter $\epsilon$

398 The reward parameter  $\epsilon_j^k$  is introduced in order to accom-  
 399 modate the heterogeneous processing capability of nodes. Certain  
 400 nodes, for example, may only be capable of processing specific  
 401 types of content, due to hardware or software constraints, while  
 402 other nodes may not be able to process any type of data. The re-  
 403 ward parameter  $\epsilon_j^k$  is used to give additional credit for a node  $j$   
 404 that can process the corresponding content  $k$ . The value of the re-  
 405 ward parameter is set as follows:  
 406

$$\epsilon_j^k = \begin{cases} 0, & \text{if } j \text{ cannot process } k \\ \sigma, & \text{if } j \text{ can process } k \text{ } (\sigma \text{ is a constant}) \end{cases}$$

407 Please note that the marginal processing gain in  $F$  already gives  
 408 credit to a Node  $j$  that is able to process content  $k$ , providing a  
 409 traffic reduction of  $k$  can be produced on  $j$ . Therefore, even in the  
 410 absence of the reward parameter, traffic is more likely to be for-  
 411 warded to nodes that are capable of processing the data in addi-  
 412 tion to merely relaying it. An example of this is illustrated in  
 413 Fig. 8(a).<sup>5</sup> However, if a Node  $j$  has the capability of processing  
 414 content  $k$  but there is currently no other traffic  $k$  routed via  $j$ , the  
 415 processing gain is zero because there is no traffic reduction. In this  
 416 instance, the reward parameter can help to ensure that traffic is  
 417 still forwarded to that Node  $j$  as shown in Fig. 8(b). Thus, although  
 418 the value of  $\sigma$  could be relatively small compared to the other pa-  
 419 rameters in  $F$ , it provides a bias to forward traffic to nodes that are  
 420 capable of processing the particular type of content in question.

#### 4.3. Candidate selection and loop avoidance

421 Communication loops can cause several problems such as traf-  
 422 fic congestion, packet loss (due to Time-To-Live expiry), and addi-  
 423 tional energy consumed in repeatedly processing and transmission  
 424 of looping messages. In RPL [6], a popular routing protocol used  
 425 in lossy wireless networks, a message header is used to detect  
 426 communication loops. RPL does not allow messages to be routed  
 427 'down' to a child node, if these are supposed to be sent 'up' to-  
 428 wards the root. If a loop is detected, the message is discarded  
 429 and a local repair is carried out. However, such a loop avoidance  
 430 scheme limits the number of neighbors that can be selected as the  
 431 next hop relay. Consequently, this limits the possibility to perform  
 432 distributed processing and to reduce the network traffic volume.  
 433

<sup>5</sup> Note that for simplicity, in this example, the link quality aware local network lifetime estimation is omitted from consideration.

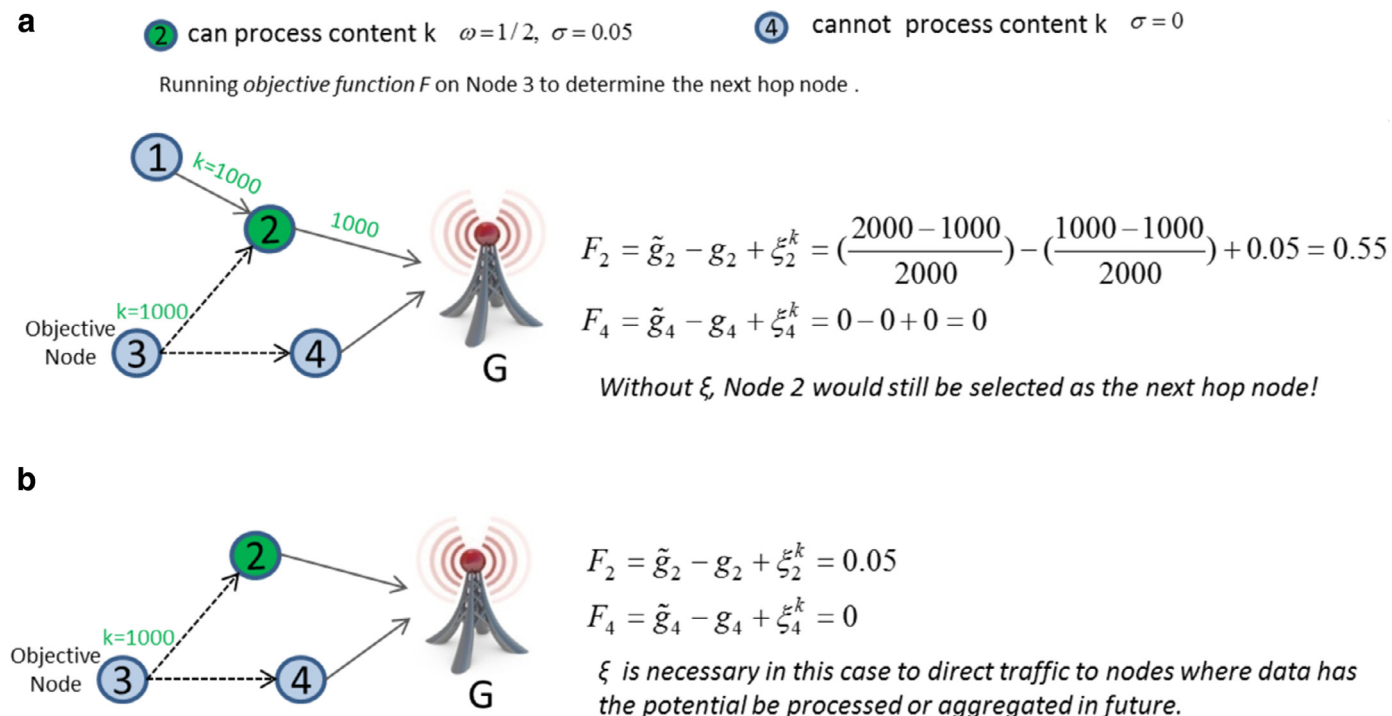


Fig. 8. Example of the benefit of  $\xi$ .

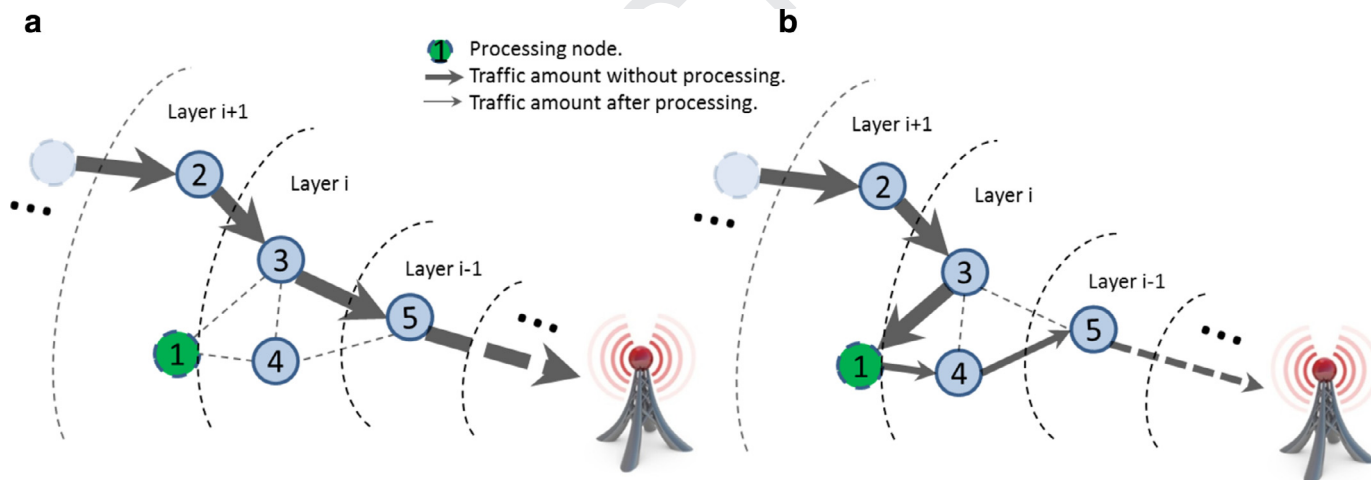


Fig. 9. Example shown the advantage of TTGF loop avoidance.

434 To overcome this limitation, we introduce the Time-To-Go-Forward  
 435 (TTGF) in order to select appropriate neighboring nodes (as candi-  
 436 date next hop nodes) that would respond to the local query mes-  
 437 sage and avoid communication loops. TTGF relaxes the restriction  
 438 introduced in RPL that traffic bound for upward nodes cannot be  
 439 routed to a downward node, provided a higher processing gain can  
 440 be achieved within the TTGF tolerance range. Fig. 9 shows an ex-  
 441 ample of the difference between the TTGF approach (Fig. 9(a)) and  
 442 the conventional RPL loop avoidance approach (Fig. 9(b)).

443 TTGF is a similar notion to the Time-To-Live (TTL) metric which  
 444 can be added to the header of the data packet. It works together  
 445 with the node layer ID, which represents the minimum number  
 446 of hops required for each node to reach the sink. Details of how  
 447 to obtain this node layer ID is described in Section 3. TTGF con-  
 448 tains two parameters: (1) the TTGF layer ID, (2) the TTGF count.  
 449 The TTGF layer ID points to the lowest node layer ID that a mes-  
 450 sages reaches. The value of TTGF layer ID is updated as the packet

451 is forwarded on the way to the sink. If a successful forward trans-  
 452 mission is made (the current/recipient node layer ID < TTGF layer  
 453 ID), the value of the TTGF layer ID is updated by the current node  
 454 layer ID. The TTGF count works as a 'count down' parameter. In  
 455 case the recipient has the same or higher node layer ID compared  
 456 to the TTGF layer ID, the message has not reached 'closer' to the  
 457 sink. Therefore, the TTGF count is reduced by one. Once the TTGF  
 458 count reaches zero, only those with a lower layer ID compared to  
 459 the objective node's layer ID can be chosen as the next hop candi-  
 460 date. The TTGF count is set to the preset default value once the  
 461 TTGF layer ID is updated.

462 By using TTGF, we allow messages to be relayed to nodes with  
 463 the same or even higher depth of the network layer within the  
 464 TTGF tolerance value, such that a proper processing node can be  
 465 found in order to aggregate data. On the other hand, if a message  
 466 that has not been forwarded any 'closer' to the sink within TTGF  
 467 hops, is forced to do so by selecting a lower layer node as the next



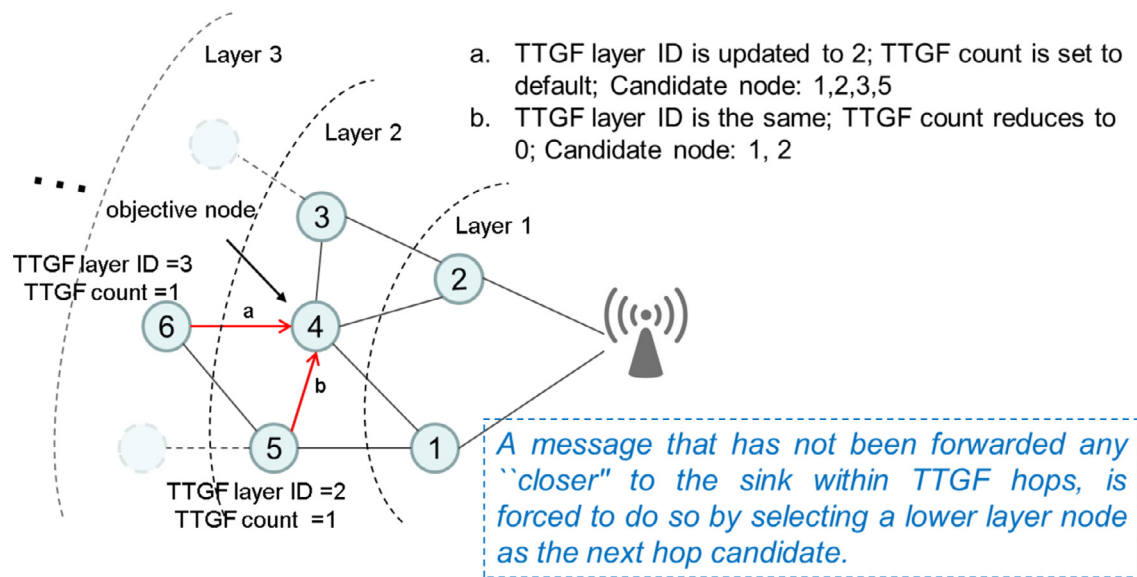


Fig. 10. Loop avoidance with TTGF.

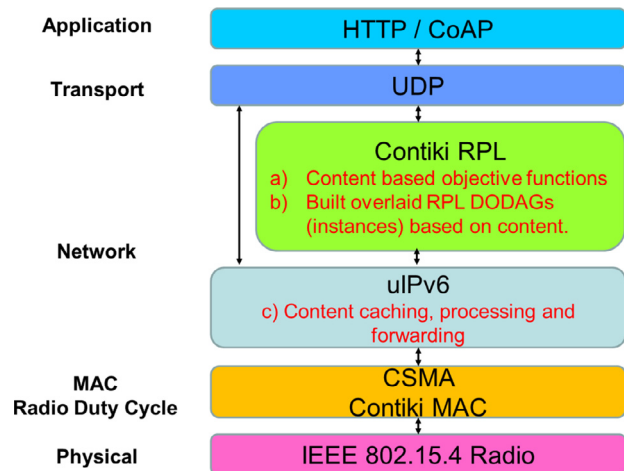


Fig. 11. The integration of CCR components into Contiki and RPL architecture.

468 hop candidate. An example of using TTGF is shown in Fig. 10. In  
469 case of event (a) shown in Fig. 10, a forward transmission is made  
470 from node 1 (layer 3) to node 4 (layer 2). Hence, the TTGF layer  
471 ID becomes 2 and TTGF count is set to default. Therefore, all the  
472 one hop neighboring nodes apart from the previous sender can be  
473 the next hop candidate for node 4. For case (b) shown in Fig. 10,  
474 the TTGF layer ID is the same while the TTGF count is reduced by  
475 1 and becomes 0 when it reaches node 4. Thus, only those with  
476 a lower layer ID (Node 5 and 6) are qualified for the candidate  
477 selection and respond to the query message.

## 478 5. CCR implementation and integration in RPL

### 479 5.1. Summary of RPL

480 The Routing Protocol for Low-power and Lossy Networks (RPL)  
481 is developed and standardized by IETF for enabling connectivity in  
482 IoT mesh networks. RPL uses a proactive process to construct and  
483 maintain a Destination-Oriented Directed Acyclic Graph (DODAG)  
484 routing topology, where the data concentrator sits at the root of  
485 the DODAG and the edges form a path from each node to the DAG  
486 root. The DODAG construction starts with the root broadcasting a

DIO (DODAG Information Object) control message. Any node received  
487 this message can choose to join the DODAG by adding the DIO sender  
488 to its parent list, and computes its rank relative to the parent node  
489 based on an objective function. It then further forwards the DIO  
490 message with updated rank information. Once the DODAG is in place,  
491 nodes can send data via their relay parents until it reaches the root.  
492 If the network is in a steady state, RPL uses a low-rate DIO beacon  
493 process controlled by Trickle timer in order to maintain the DODAG  
494 routing topology. However, RPL would temporarily increase the DIO  
495 sending frequency by resetting the trickle timer if network inconsistencies  
496 were detected. This process allows RPL to dynamically adjust its control  
497 operations and reduces unnecessary control overheads. 499

### 500 5.2. CCR's operation in Contiki RPL

In the following, the integration of CCR components into the  
501 industrial RPL protocol is described. The detailed system architecture  
502 is shown in Fig. 11, where our contributions are highlighted, notably  
503 we have: a) Developed a content based objective function for the RPL  
504 protocol; b) Enabled multiple RPL instances on the same RPL root,  
505 such that messages with different content types are routed via  
506 different RPL DODAG instances. c) Caching, processing and forwarding  
507 functions are added to the network layer to facilitate in-network data  
508 aggregation. Details are described below. 509

510 There are a few ways to implement CCR, one way is to specify a  
511 content Byte in the packet routing header, and the procedures described  
512 in Section 4 can be used. However, a standard based implementation  
513 is more promising. Therefore, we adopt the existing Contiki RPL  
514 standard as a baseline, which is augmented with more functionality  
515 without affecting backwards compatibility. 515

516 To meet Contiki RPL's implementation style, we revised CCR's  
517 messaging exchange procedure and adopted the existing DIO and  
518 DAO (DODAG Destination Advertisement Object) control messages  
519 proposed in RPL. In addition, since RPL supports multi-topology  
520 routing over the same physical mesh network by using an instance-id,  
521 we assign instance-id to each content type and create multiple  
522 overlaid routing topologies (DODAGs) based on content. 522

523 For each content (RPL instance)  $c$ , the root node first starts  
524 advertising the information about the DODAG graph using the DIO  
525 message. Any node within the listening vicinity receives the message,  
526 and then it processes the message and makes a decision

527 whether or not to join the graph according to the objective func-  
 528 tion. Node rank is computed representing the relative position in  
 529 the DODAG with respect to the root. For simplicity, the objective  
 530 function in (3) is simplified for CCR implementation and the node  
 531 rank for each instance  $c$  can be calculated as per (9).

$$R_{Node}(c) = R_{parent}(c) - N_{content}(c) * \omega + O_{rank}(c) * \eta + BaseHop \quad (9)$$

532 where  $R_{parent}$  is a parent node's rank;  $N_{content}$  is the total num-  
 533 ber of child nodes associated with the parent node for the same  
 534 content  $c$  (parent node is inclusive if it is also the source node of  
 535 content  $c$ ). This means if a parent node having more children for  
 536 the same content, it would have a larger value of  $N_{content}$ , hence a  
 537 lower rank (a better parent) in the DODAG graph;  $O_{rank}$  stands for  
 538 any other objective function (3) related parameters, for instance,  
 539 ETX or Residual battery level etc.;  $\omega$  and  $\eta$  are weighting param-  
 540 eters; and BaseHop is a constant. If BaseHop is not equal to 0, the  
 541  $R_{Node}$  increases by adding more hops.

542 An example of CCR based multi-DODAG construction is shown  
 543 in Fig. 12, where Nodes 2, 4, 7, generates content A, Nodes 3, 5, 6,  
 544 generate content B, and Node 8 generates both content A and con-  
 545 tent B. The initial single DODAG routing topology without CCR is  
 546 shown in Fig. 12(1). Now, when we apply CCR, different instance-  
 547 ids are given to content A and content B, hence the DODAG shown  
 548 in Fig. 12(1) can be separated into two as shown in Fig. 12(2) and  
 549 (3). For simplicity, we assume  $O_{rank} = 0$ , root rank is 10, and Base-  
 550 Hop is set to 4. Each parent will pass its own rank ( $R_{parent}$ ) along  
 551 with the Content factor ( $N_{content}$ ) in the DIO message. Let us take  
 552 content A for example as shown in Fig. 12(3). Since the root node  
 553 only has Node 2 to provide content A messages, the rank of Node  
 554 2  $R_2(A)$  can be calculated by using (9) as  $R_2(A) = R_{root}(A) - 1 + 4 =$   
 555 13. Similarly, the rank of Node 4 and Node 5 can be calculated ac-  
 556 cordingly. Now, in order to choose the best parent for Node 8, it  
 557 needs to calculate its rank based on whether to choose Node 4 or  
 558 Node 5 as its parent. Since, there would be 3 nodes (Nodes 4, 7,  
 559 8) sending content A messages to Node 4, hence  $N_{content}(A) = 3$ .  
 560 In contrast, Node 5 would only have Node 8 to send content A  
 561 packets if it was chosen as parent, therefore  $N_{content}(A) = 1$ . Obvi-  
 562 ously, Node 4 is a better parent compared with Node 5 based on  
 563 the objective function. As a result, Node 8 will switch its parent  
 564 from Node 5 to Node 4 as shown in Fig. 12(5). Same parent se-  
 565 lection process is carried out for Content B in Fig. 12(2) and (4).  
 566 Eventually, two distinctive DODAGs for content A & B are formed  
 567 as shown in Fig. 12(6).

### 568 5.3. CCR core modules

569 **Memory allocation:** a set of memory blocks is statically allocated  
 570 for buffers, caches, and other data structure to handle CCR's com-  
 571 munication.

572 **Content entry:** this module includes three main functions,  
 573 Node\_Has\_Content(), \*Content\_Type\_Get() and Node\_Add\_  
 574 Content(). The first function checks whether a parent Node has  
 575 already cached the same content of a received message from its  
 576 child. If so, the second function is called to retrieve the pointer  
 577 pointing to the corresponding content in the memory. Otherwise,  
 578 the Node\_Add\_Content() is used to allocate memory to the new  
 579 content. Due to memory limitation of the Hardware platform, the  
 580 maximum number of content is set to 3 in this implementation.

581 **Content caching:** a content table is built with a unique index  
 582 assigned to each content object. The received packet payload is  
 583 then copied to the content table with a matching to the corre-  
 584 sponding content type.

585 **Content processing and forwarding:** cached data for each content  
 586 will be processed if the parent node receives packets from its chil-  
 587 dren or the maximum number of message stored in the buffer for

**Table 1**  
Energy consumption of different operations per Byte.

Operations	Energy consumption ( $\mu$ J)
Transmission	9.72
Reception	8.22
Flash write	0.445
Flash read	0.315
Data aggregation	0.0011

the corresponding content is reached, or a timeout() is triggered. 588  
 The processed data will be forwarded based on the destination IP 589  
 address and destination port. 590

## 591 6. Performance evaluation

### 592 6.1. Simulation results

593 A simulation based study was first carried out in order to evalu-  
 594 ate the performance of the proposed CCR protocol with the con-  
 595 ventional methods. A global network lifetime maximization tree  
 596 algorithm [27] (referred to as *Static Tree* hereafter) and the tradi-  
 597 tional centralized processing scheme (referred to as *Central* here-  
 598 after) were chosen as benchmarks.

599 The Static Tree is a centralized algorithm which pre-constructs  
 600 a maximum-lifetime data gathering tree before the network starts  
 601 to operate. In order to achieve a fair comparison, we added the  
 602 data aggregation to the Static Tree approach. In addition, since  
 603 global knowledge is required to perform the optimization for Static  
 604 Tree, which can be very time consuming to re-compute the opti-  
 605 mal tree each time there is a change in the network such as  
 606 node/link failures. To mitigate this issue, we slightly modified the  
 607 static tree algorithm to adapt to such failure cases, and apply a  
 608 simple but fast recovery mechanism to randomly choose the next  
 609 hop node with a lower layer ID if a failure event happens. On the  
 610 other hand, the central algorithm first gathers all the data at the  
 611 sink and then carries out processing to compute the results.

#### 612 6.1.1. Simulation parameters

613 Unless specified otherwise, a network deployment compris-  
 614 ing of 200 nodes with nodes being uniformly distributed with a  
 615  $200 \times 200 \text{ m}^2$  area was assumed. Three applications with hetero-  
 616 geneous traffic rates were considered in the simulations. Nodes  
 617 were assumed to have unequal energy levels at the startup time  
 618 in the range 4–6 J. The TTGF count was set to 2 and the con-  
 619 trol packet size was assumed to be 500 bits.  $p_{default}$  was set to  
 620 0.05 and the value of  $\beta$  was set to 2. A simple data aggrega-  
 621 tion function which computes the maximum and the average of  
 622 the sensed values was considered in the simulations. A variable  
 623 data aggregation rate  $\omega = \frac{1}{M}$  was used, where  $M$  is the total num-  
 624 ber of messages received for the same application on a process-  
 625 ing node. Tmote Sky node was chosen as our basic node model  
 626 which is equipped with an MSP430 processor and CC2420 radio  
 627 chip. The energy consumed by the different operations (per Byte)  
 628 for the Tmote Sky platform are adopt from [31], [32] and listed in  
 629 Table 1. Finally, the performance of the proposed CCR algorithm  
 630 was compared with a centralized lifetime maximization tree algo-  
 631 rithm [27] (referred to as *Static Tree* hereafter) and the traditional  
 632 centralized processing scheme (referred to as *Central* hereafter). All  
 633 simulation results were averaged from 200 test runs which show  
 634 99% confidence interval with about mean-value  $\pm 10\%$  precision.  
 635 The implementation experiments were run for more than 40 times  
 636 which show 95% confidence interval within  $\pm 10\%$  of the sample  
 637 mean.

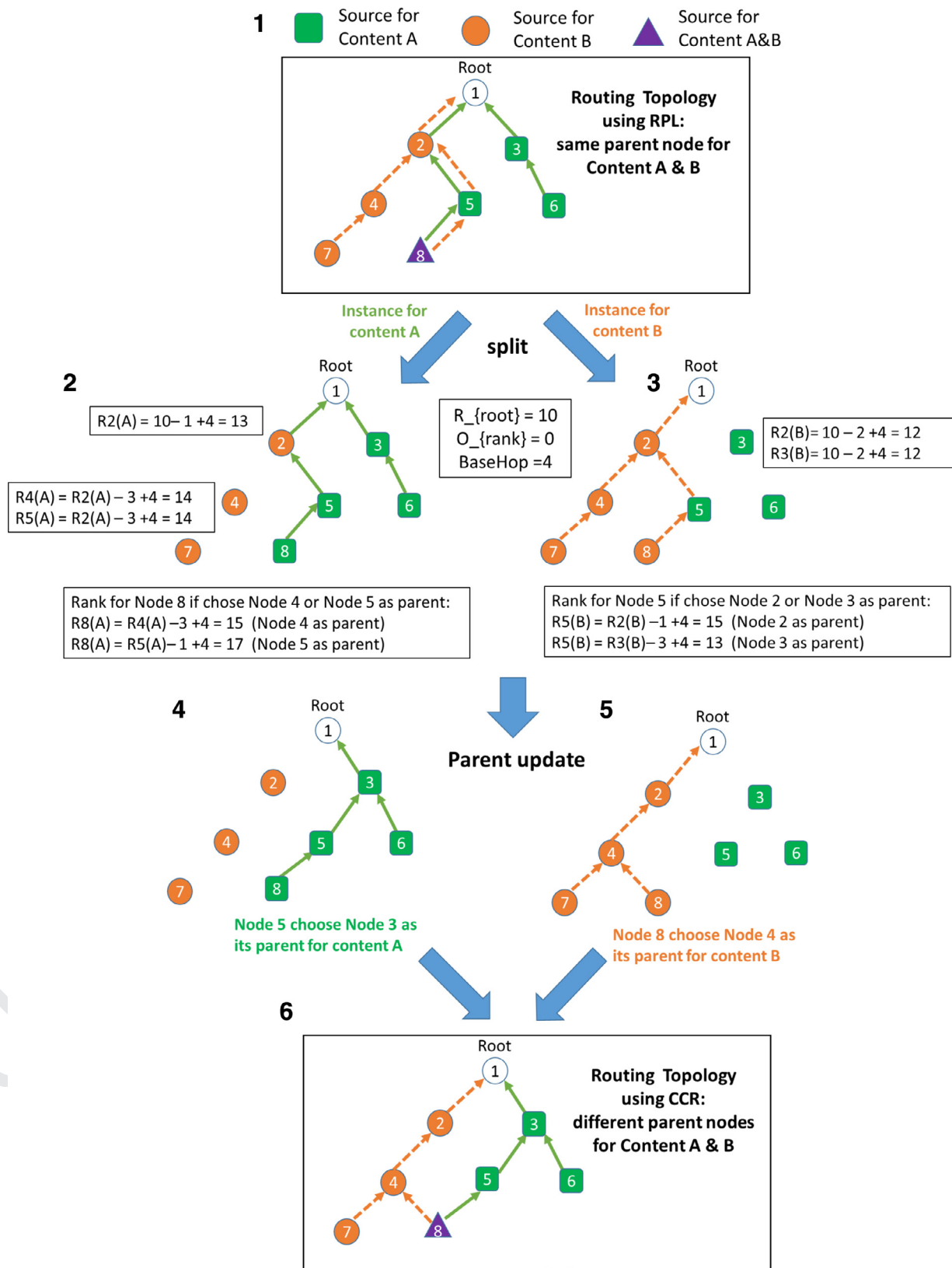


Fig. 12. Mutil-DODAG graphs building process based on content types.

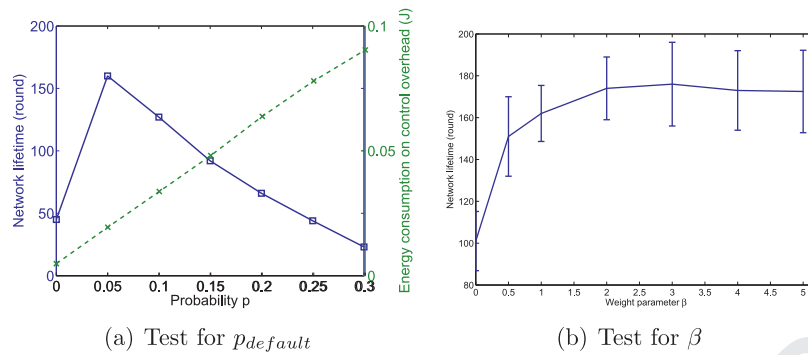
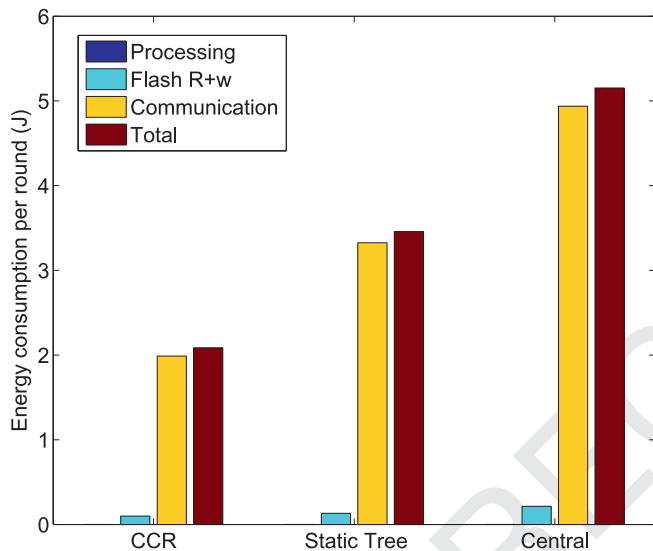
Fig. 13. Impact of  $p$  and  $\beta$  on network lifetime.

Fig. 14. Energy consumption per round for different processes.

### 6.1.2. Impact of $p_{default}$ and $\beta$ on lifetime

To begin with, simulations were run to determine the probability  $p_{default}$  of executing the objective function  $F$ , and the weight parameter  $\beta$  to decide the tradeoffs between the processing gain and the local lifetime gain.  $p_t = p_{default}$  when the network is in a stable status. Intuitively, a larger value of  $p_{default}$  gives more chances for each node to select the best hop candidate in terms of having a higher processing gain as well as a balanced lifetime. However, as seen from Fig. 13(a), the network lifetime first increases when  $p_{default}$  is set to 0.05, but then it drops very quickly as the value of  $p_{default}$  further increases. This stems from the fact that when  $p_{default}$  increases, more energy is spent on the control overhead to gather local information in order to execute  $F$ . As evident from Fig. 13(a), the energy consumption related to the increased control overhead also increases linearly with  $p_{default}$  which implies that the node energy depletes.

A suitable value of  $\beta$  is also needed as it has an impact on the local lifetime gain. A large value of  $\beta$  puts more weight on the local network lifetime gain which consequently produces a smaller value of  $F$  for the bottleneck node. However, when  $\beta$  is large enough to avoid overloading the bottleneck node, this increase of  $\beta$  value has no further impact on the network lifetime as evident from Fig. 13(b).

Therefore, application or network specific configurations might be required before the network start to operate. Nevertheless, such simple configuration is acceptable by the industry, for example, the Trickle timer parameter can be tuned in the RPL protocol in or-

der to achieve the best performance result. Please note that in the following experiments, corresponding  $p_{default}$  and  $\beta$  values determined in this section are used.

### 6.1.3. Energy consumptions

Simulations were run to identify the contribution of each of the data processing, flash read/write and communication operations to the total energy consumption. Fig. 14 shows the per round energy consumption of processing, flash read/write and communication operations and, the sum total of these. It is evident from this figure that the energy consumed by communications significantly dominates the energy consumed by the other operations. The central algorithm gathers all the data at the sink and then carries out processing as a result of which it exhibits the highest communication cost. By taking advantage of content-centric data aggregation to reduce the volume of data that needs to be transported, CCR saves more than half of the energy spent on communication in comparison to the Central approach, about a third in comparison to Static tree. Although in-network data aggregation is enabled in Static Tree, it still incurs higher communication cost in comparison to the proposed algorithm. This is because it employs a centralized routing optimization approach, i.e. tree does not adapt to changes in the underlying network (traffic dynamics). Global knowledge of the network is needed to perform the optimization. In a dynamic network environment, it can be time consuming to recompute the optimal tree each time there is a change in the network such as node/link failures, or arrival of a new application. Thus, the performance of the pre-optimized network topology in the Static Tree approach degrades over time. Furthermore, since the processing cost is too small to be spotted in Fig. 14, we point out that the Central approach spent only 31  $\mu$ J of energy on processing. This is only half of the processing cost compared with CCR and Static tree. The key point to take note of here is that even a small increase in processing cost for CCR and Static tree translates to large increase in energy saving gains on communication.

### 6.1.4. Network lifetime

The network lifetime is defined as the time duration between when the network starts to operate until the first node dies due to energy depletion. As evident from this Fig. 15(a), CCR provides a significant increase in network lifetime compared with the other two. Furthermore, we observe that CCR has a smaller gap when the network is scaled from 100 nodes to 300 nodes. This boils down to the ability of CCR to reduce considerable amount of traffic in the network as a result of using content-centric data aggregation. Additionally, Fig. 15(b) shows the total energy spent on retransmissions per simulation round. As evident from this figure, CCR spends the least amount of energy on retransmissions. This is attributed to its ability to form a more reliable routing topology by taking link quality into account. The central algorithm has the highest energy

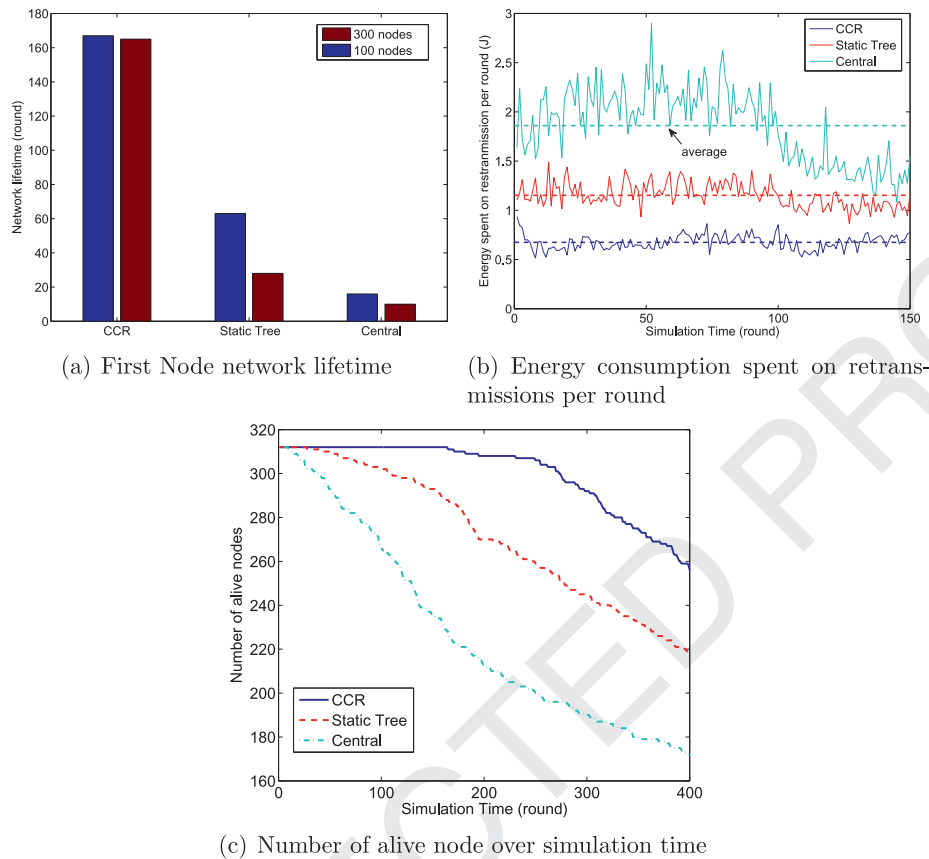


Fig. 15. Network lifetime comparison.

713 spent on retransmissions due to heavy traffic on links. However,  
 714 it drops significantly at the latter stage. This stems from the fact  
 715 that the number of alive nodes in the network is significantly de-  
 716 creased, hence less traffic is generated in the network compared  
 717 to the other two. Finally, the number of alive nodes against simu-  
 718 lation time is shown in Fig. 15(c). Clearly, CCR conserves more  
 719 energy resources for nodes which is vital for resource constrained  
 720 devices.

#### 721 6.1.5. Graphical network traffic comparison

722 Fig. 16 provides visualized traffic maps for a simulated network  
 723 with nodes generating three different types of contents. The line  
 724 width in the traffic map represents the volume of data flowing  
 725 through that link, i.e., the thicker the line, the higher the volume  
 726 of traffic flowing through it. Nodes marked by red color in each con-  
 727 tent traffic map are those that can process the corresponding con-  
 728 tent. By using CCR, it can be observed that traffic flows of the same  
 729 content are more likely to be routed to those red processing nodes  
 730 and correlated data is more likely to be aggregated within the net-  
 731 work resulting a much less traffic amount as shown in Fig. 16.

732 Fig. 17 provides traffic map comparison at different network op-  
 733 eration time instances. The 'x' mark indicates a dead node that has  
 734 already depleted its energy. We can see that the Central approach  
 735 has much heavier communication traffic compared with CCR. In  
 736 addition, since the nodes in the area that are closer to the sink  
 737 need to relay information for those located in the outer region.  
 738 Massive traffic can be observed at the centre of the network for  
 739 the Central method. This could easily cause the hot-spot problem,  
 740 while CCR and Static tree have much less communication data vol-  
 741 ume after aggregation. Furthermore, by observing the number of  
 742 dead nodes in Fig. 17, we can clearly tell that CCR performs much

Table 2

Experiment setup.

Experiment setup	Parameters
High data rate	1 Packet per second per node
Low data rate	1 Packet per 5 seconds per node
Traffic type	CBR
Number of nodes	10(3Hops), 15(4Hops), 20(5Hops)
Types of contents	2
Maximum cached messages per content	3
Baseline benchmark	RPL

743 better in conserving node energy as well as in providing full net-  
 744 work coverage.

#### 745 6.2. Implementation results

746 In this section, we experiment on the evaluation of CCR's per-  
 747 formance in Contiki Cooja Emulator based on the TelosB (also  
 748 known as Tmote Sky) Platform. A screen shot of the emulator is  
 749 shown in Fig. 18 and details of the experiment setup are shown  
 750 in Table 2. Since it is not straight forward to implement the *Static*  
 751 *Tree* in contiki cooja, we choose the *RPL* standard as the main com-  
 752 petitor in our implementation based experiments. Similar to the  
 753 *Central* approach, *RPL* does not process data while routing packets.

754 Fig. 19 presents the number of average transmitted packets over  
 755 a 10 s of period in the network. It can be observed that CCR is  
 756 able to significantly reduce the amount of traffic. As a results, CCR  
 757 spends less energy on communication and prolongs network life-  
 758 time as shown in Fig. 20. Although it can be noticed that CCR  
 759 outperforms *RPL* in extending the network lifetime, the perfor-  
 760 mance gain is reduced compared with our simulation results. This

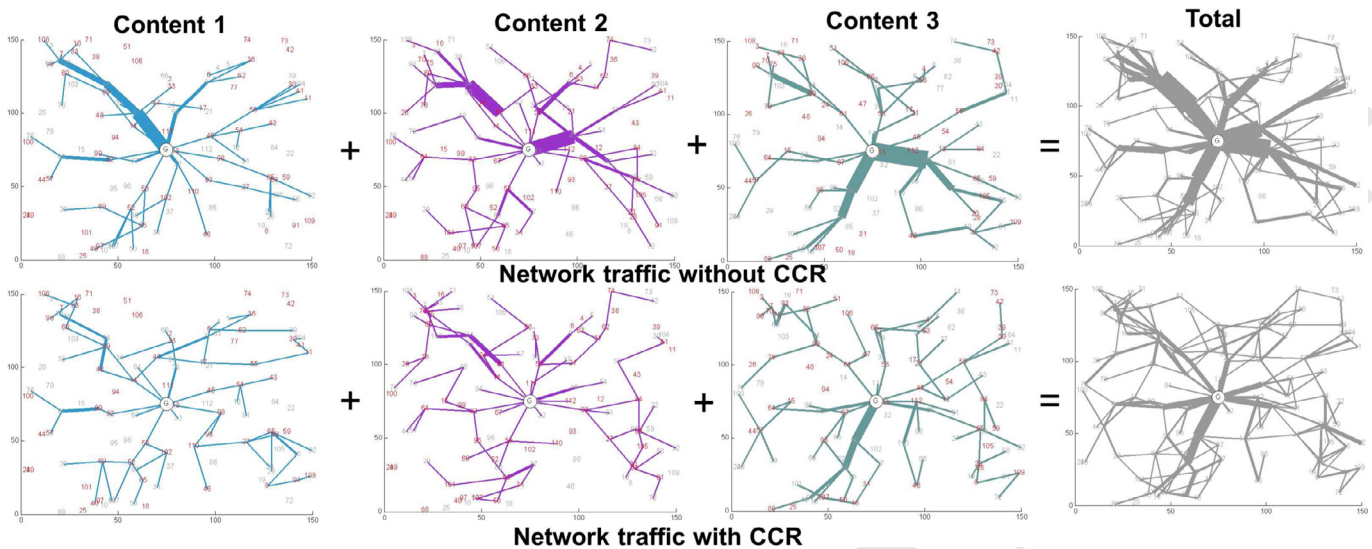


Fig. 16. Network traffic maps with 3 different contents. (For interpretation of the references to color in this figure, the reader is referred to the web version of this article).

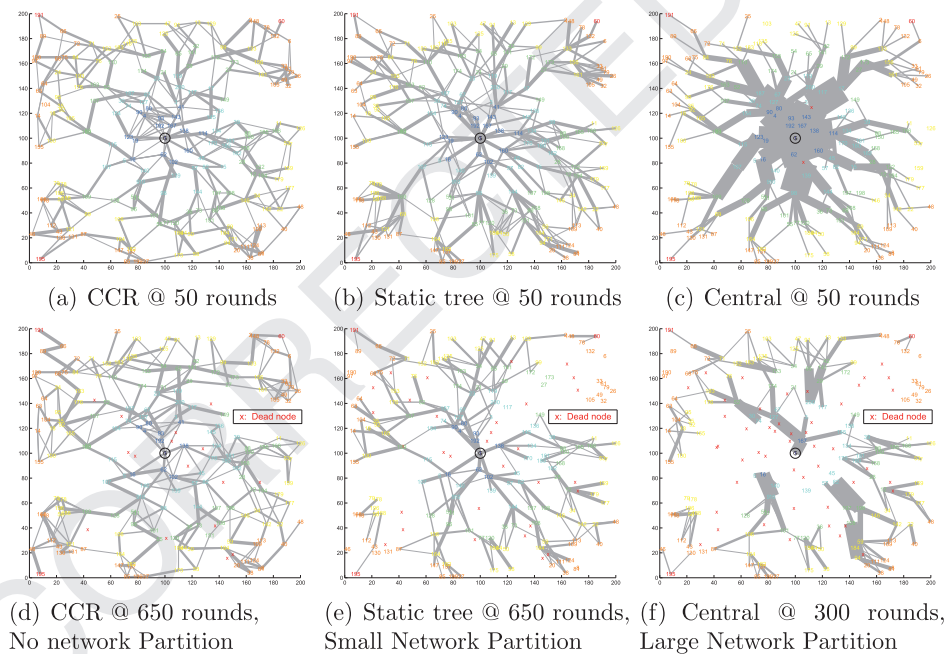


Fig. 17. Graphic comparison of traffic maps at different time instances.

761 is mainly due to the reason that we adopted the RPL based mes- 762  
 763 saging in order to make it compliant with the standard. However, this incurs additional costs on control overhead.

764 Two additional experiments were conducted in this implemen- 765  
 766 tation evaluation, which could not be performed in the previous 767  
 768 simulation based tests. We first measure the average packet delay. In this test, a special message is generated on the farthest leaf 769  
 770 node, the average reception time on the root node is recorded. In order to have a correct and fair measurement of network latency, 771  
 772 this special message is not cached in CCR as this incurs additional 773  
 774 waiting time, while the other messages are cached and processed 775  
 776 in the network. The results obtained are shown in Fig. 21.

777 Although the network latency increases when the number of 778  
 779 hops increases in the case of both approaches (CCR & RPL), CCR 780  
 781 outperforms RPL in both low data rate case and high data rate 782  
 783 case. This is because the network is less congested by using CCR, 784  
 785 therefore a low network latency can be achieved. We also observe 786  
 787 that the magnitude of the improvement increases with an increase 788  
 789

790 in the scale of the network. With 5 Hops (20 nodes) and high 791  
 792 data rate setting, CCR can provide as much as twice the reduc- 793  
 794 tion in network latency. This indicates the scalability of CCR in 795  
 796 dense deployments. We further measured the packet delivery ra- 797  
 798 tio and the outcome is illustrated in Fig. 22. RPL has a rapid per- 799  
 800 formance degradation when the number of nodes increase to 20, 801  
 802 only 46% and 20% of the messages will eventually reach the sink 803  
 804 in the low data rate and high data rate case, respectively. This 805  
 806 is because the central area is highly congested due to heavy net- 807  
 808 work traffic, which RPL is not able to accommodate. In contrast, CCR still 809  
 810 achieves over 90% of PDR in the low data rate case with 20 nodes 811  
 812 and 60% of PDR in high data rate case. 813

6.3. CCR demonstration

791 Finally, we ported our implementation codes to the real hard- 792  
 793 ware (TelosB node) and developed a Demo. Since it is very 794  
 795 challenging to deploy a large-scale multi-hop network with real 796  
 797

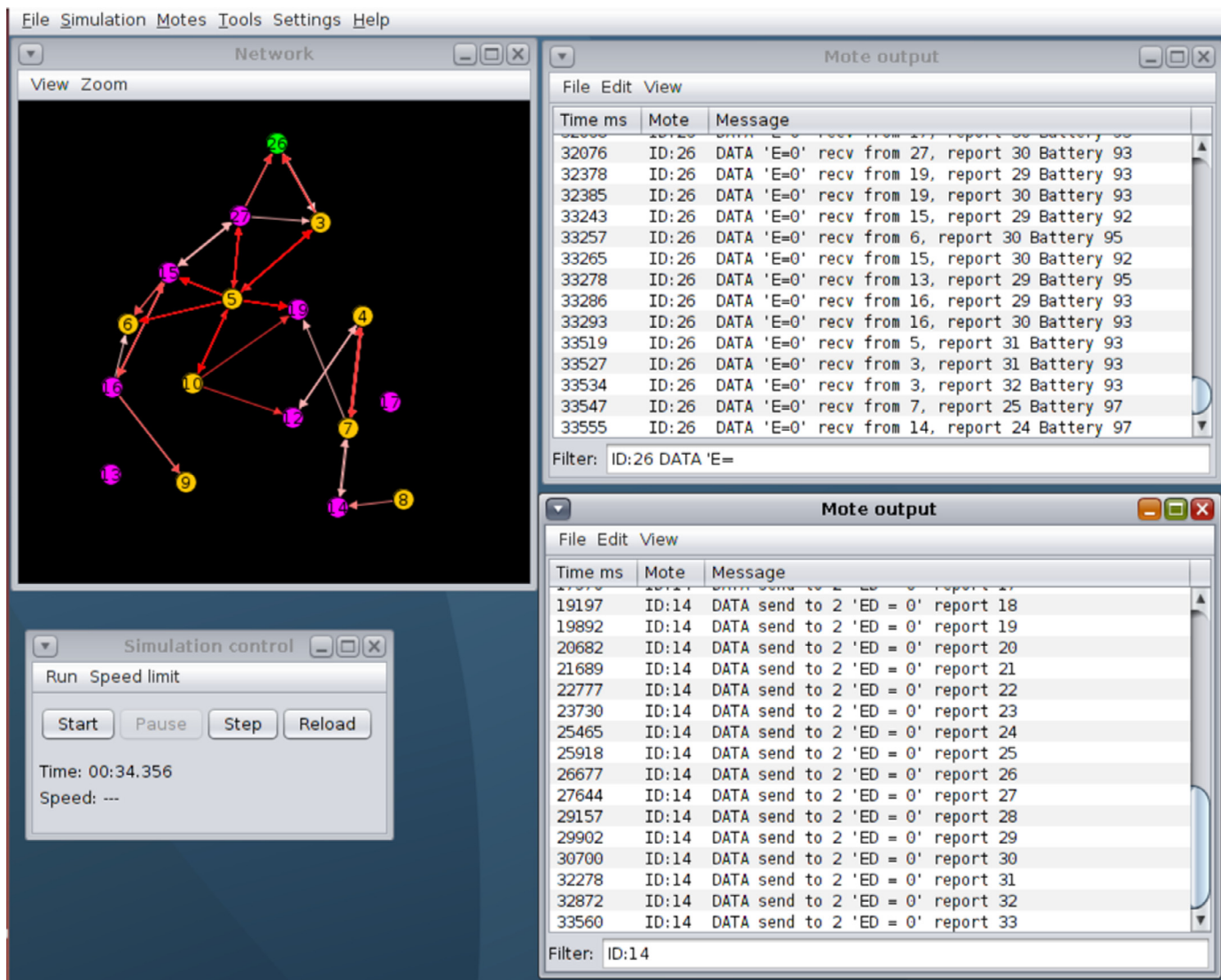


Fig. 18. CCR's evaluation on Contiki Cooja.

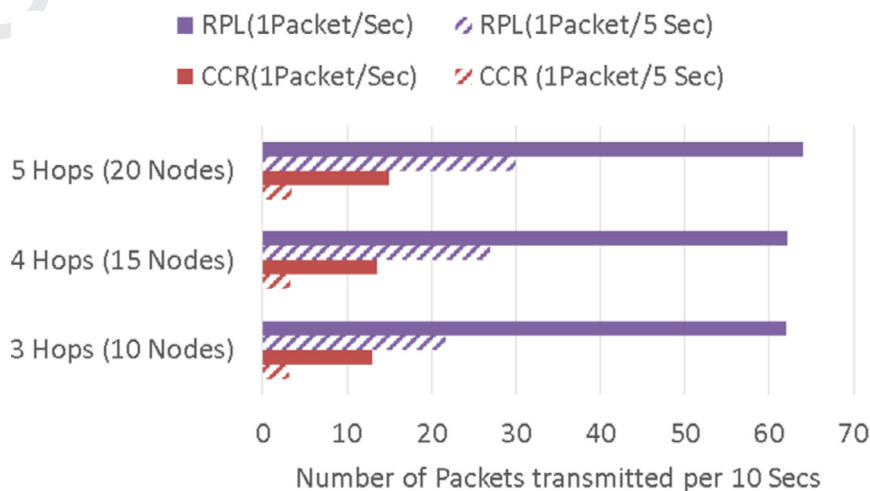


Fig. 19. Experimental results – aggregation gain.

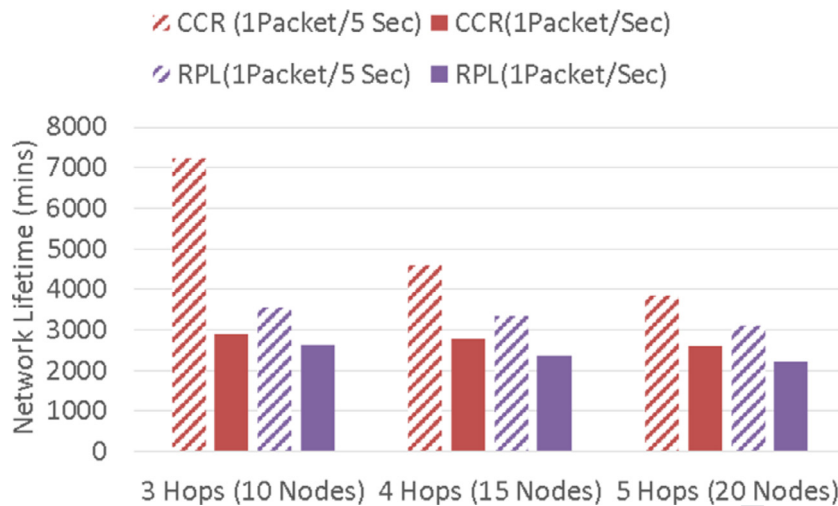


Fig. 20. Experimental results – network lifetime.

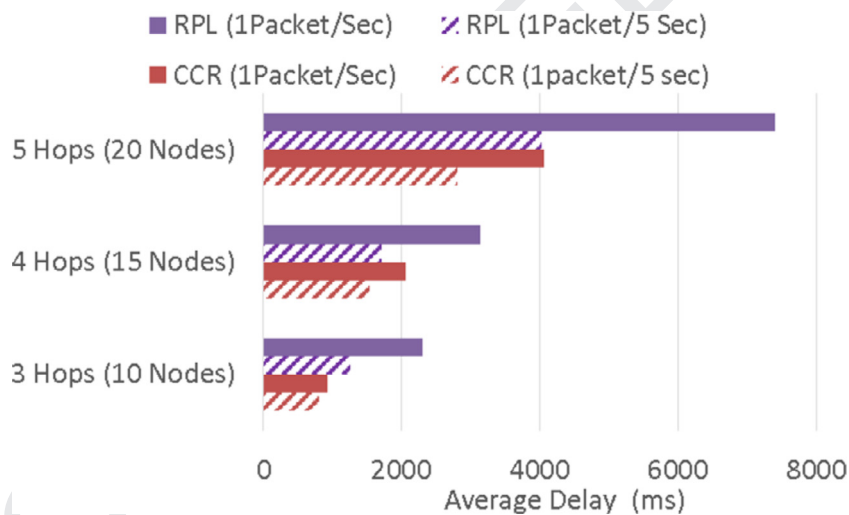


Fig. 21. Experimental results – network latency.

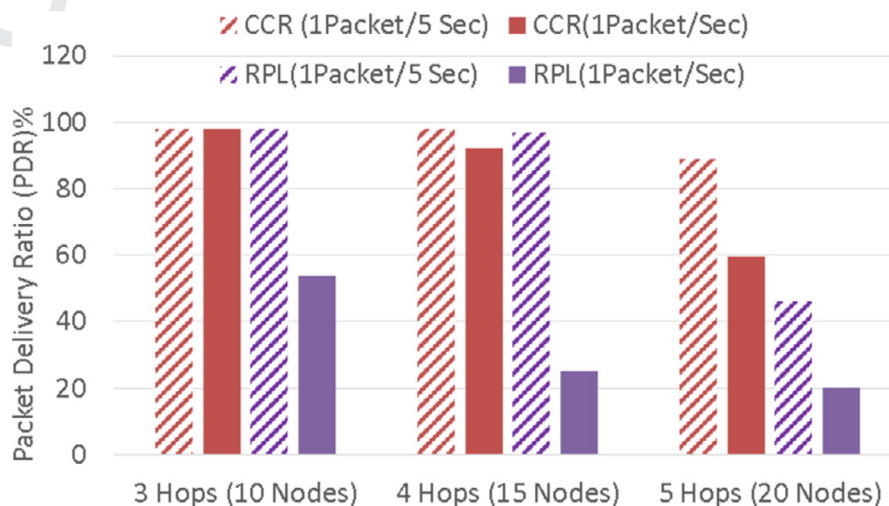


Fig. 22. Experimental results – packet delivery ratio.



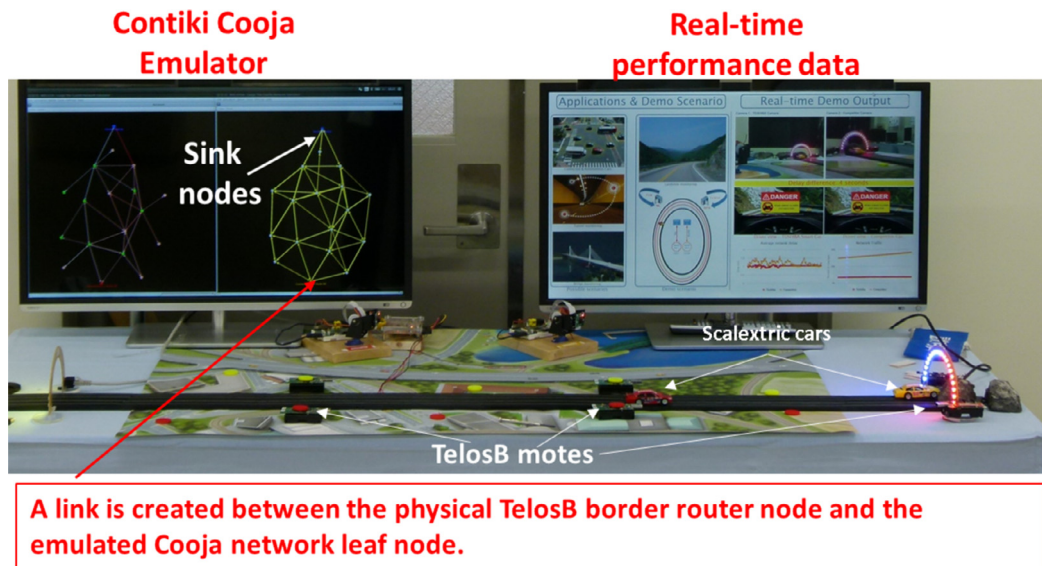


Fig. 23. CCR demo setup.

795 hardware nodes, as a first step we found a hybrid solution with  
 796 a Contiki Cooja emulator emulating a large-scale mesh network  
 797 along with a few physical nodes to form the outer part of the mesh  
 798 network. Both the physical node and emulated node are running  
 799 the same CCR code. The boarder router of the physical network is  
 800 connected to one of the leaf nodes emulated in the Contiki Cooja  
 801 emulator. Hence, all packets sent by the telosB motes will route  
 802 through both the small scale real mesh network and the emu-  
 803 lated large-scale wireless mesh network. By such approach, we can  
 804 demonstrate CCR technological benefit for a large scale mesh net-  
 805 work, a demo setup picture can be seen in Fig. 23. We have suc-  
 806 cessfully showcased the CCR demo in various occasions including  
 807 Venturefest Bristol and Bath, 2015.

## 808 7. Conclusion

809 In this paper, we proposed and studied the performance of an  
 810 efficient data aggregation and reliable data delivery scheme CCR  
 811 for a deployment scenario where data from the IoT network end-  
 812 points such as sensors have to traverse over wireless lossy links on  
 813 the way to the other endpoint hosting the IoT application. In par-  
 814 ticular, CCR is a distributed approach which considers the traffic  
 815 reduction gain achieved through content-centric data aggregation  
 816 when routing traffic over reliable communication links by incor-  
 817 porating link quality information. Based on the content of a mes-  
 818 sage, each node constructs a separate routing entry for each con-  
 819 tent type by running the proposed novel objective function; the  
 820 key idea being to route heterogeneous types of content via selected  
 821 reliable communication links to nodes which are capable of aggre-  
 822 gating and processing the information before forwarding the sum-  
 823 mary information. This greatly reduces redundant communication  
 824 traffic and reduces retransmissions as a positive side-effect. Both  
 825 simulation and implementation results confirm that CCR can sig-  
 826 nificantly extend the network lifetime, reduce network latency and  
 827 improve communication reliability.

828 For future work, hardware motes using the CCR protocol will  
 829 be deployed in our office premises in order to collect more data.  
 830 In addition, the impact of the number of content types will be in-  
 831 vestigated with the support of new hardware with larger memory.  
 832 Last but not the least, technologies such as data mining, fuzzy logic  
 833 will be explored to support in-network processing. We expect the  
 834 performance of CCR to improve further with the implementation

of more advanced processing functions and a better content defi- 835  
 nition supporting more content types in the network. 836

## Uncited References 837

Ref. [9],[16],[19],[20] 838

## References 839

- [1] D. Datla, X. Chen, T. Tsou, S. Raghunandan, S. Hasan, J. Reed, C. Dietrich, T. Bose, B. Fette, J. Kim, Wireless distributed computing: a survey of research challenges, *IEEE Commun. Mag.* 50 (1) (2012) 144–152, doi:10.1109/MCOM.2012.6122545. 840
- [2] J. Yick, B. Mukherjee, D. Ghosal, Wireless sensor network survey, *Comput. Netw.* 52 (12) (2008) 2292–2330. 841
- [3] E. Fasolo, M. Rossi, J. Widmer, M. Zorzi, In-network aggregation techniques for wireless sensor networks: a survey, *IEEE Wirel. Commun.* 14 (2) (2007) 70–87, doi:10.1109/MWC.2007.358967. 842
- [4] Y. Jin, P. Kulkarni, S. Gormus, M. Sooriyabandara, Content centric and load-balancing aware dynamic data aggregation in multihop wireless networks, in: Proceedings of the IEEE 8th International Conference on Wireless and Mobile Computing, Networking and Communications (WiMob), 2012. 843
- [5] C. Alvarado, J. Teevan, M.S. Ackerman, D. Karger, Surviving the Information Explosion: How People Find Their Electronic Information, MIT, USA, 2003. 844
- [6] T. Winter, P. Thubert, et al, Rpl: Ipv6 Routing Protocol for Low-power and Lossy Networks, (rfc 6550), <http://www.ietf.org/rfc/rfc6550.txt>, 2012. 845
- [7] A. Dunkels, B. Gronvall, T. Voigt, Contiki – a lightweight and flexible operating system for tiny networked sensors, in: Proceedings of the 29th Annual IEEE International Conference on Local Computer Networks, 2004. 846
- [8] CCNx Project, <http://www.ccnx.org/> 847
- [9] G. Mishra, M. Dave, A review on content centric networking and caching strategies, in: Proceedings of the 2015 Fifth International Conference on Communication Systems and Network Technologies (CSNT), 2015, pp. 925–929, doi:10.1109/CSNT.2015.119. 848
- [10] G. Xylomenos, C. Ververidis, V. Siris, N. Fotiou, C. Tsilopoulos, X. Vasilakos, K. Katsaros, G. Polyzos, A survey of information-centric networking research, *IEEE Commun. Surv. Tutor.* 16 (2) (2014) 1024–1049, doi:10.1109/SURV.2013.070813.00063. 849
- [11] R. Rajagopalan, P. Varshney, Data-aggregation techniques in sensor networks: a survey, *IEEE Commun. Surv. Tutor.* 8 (4) (2006) 48–63, doi:10.1109/COMST.2006.283821. 850
- [12] S. Lindsey, C. Raghavendra, K. Sivalingam, Data gathering algorithms in sensor networks using energy metrics, *IEEE Trans. Parallel Distrib. Syst.* 13 (9) (2002) 924–935, doi:10.1109/TPDS.2002.1036066. 851
- [13] H.-C. Lin, F.-J. Li, K.-Y. Wang, Constructing maximum-lifetime data gathering trees in sensor networks with data aggregation, in: Proceedings of the 2010 IEEE International Conference on Communications (ICC), 2010, pp. 1–6, doi:10.1109/ICC.2010.5502286. 852
- [14] H.O. Tan, I. Körpeoğlu, Power efficient data gathering and aggregation in wireless sensor networks, *SIGMOD Rec.* 32 (4) (2003) 66–71, doi:10.1145/959060.959072. 853
- [15] J. He, S. Ji, Y. Pan, Y. Li, Constructing load-balanced data aggregation trees in probabilistic wireless sensor networks, *IEEE Trans. Parallel Distrib. Syst.* 25 (7) (2014) 1681–1690. 854

- 885 [16] B. Zhang, W. Guo, G. Chen, J. Li, In-network data aggregation route strategy  
886 based on energy balance in WSNs, in: Proceedings of the 2013 11th Interna-  
887 tional Symposium on Modeling Optimization in Mobile, Ad Hoc Wireless Net-  
888 works (WiOpt), 2013, pp. 540–547.
- 889 [17] S. Ji, J.S. He, Y. Pan, Y. Li, Continuous data aggregation and capacity in proba-  
890 bilistic wireless sensor networks, *J. Parallel Distrib. Comput.* 73 (6) (2013) 729–  
891 745.
- 892 [18] W. Heinzelman, A. Chandrakasan, H. Balakrishnan, An application-specific pro-  
893 tocol architecture for wireless microsensor networks, *IEEE Trans. Wirel. Com-  
894 mun.* 1 (4) (2002) 660–670, doi:10.1109/TWC.2002.804190.
- 895 [19] O. Younis, S. Fahmy, Heed: a hybrid, energy-efficient, distributed clustering ap-  
896 proach for ad hoc sensor networks, *IEEE Trans. Mob. Comput.* 3 (4) (2004)  
897 366–379, doi:10.1109/TMC.2004.41.
- 898 [20] M. Ye, C. Li, G. Chen, J. Wu, Eecs: an energy efficient clustering scheme in  
899 wireless sensor networks, in: Proceedings of the 24th IEEE International Per-  
900 formance, Computing, and Communications Conference, 2005 (IPCCC 2005),  
901 2005, pp. 535–540, doi:10.1109/PCCC.2005.1460630.
- 902 [21] D. Wei, Y. Jin, S. Vural, K. Moessner, R. Tafazolli, An energy-efficient cluster-  
903 ing solution for wireless sensor networks, *IEEE Trans. Wirel. Commun.* 10 (11)  
904 (2011) 3973–3983, doi:10.1109/TWC.2011.092011.110717.
- 905 [22] Y. Abidy, B. Saadallahy, A. Lahmadi, O. Festor, Named data aggregation in wire-  
906 less sensor networks, in: Proceedings of the 2014 IEEE Network Operations and  
907 Management Symposium (NOMS), 2014, pp. 1–8.
- 908 [23] L. Villas, A. Boukerche, H. Ramos, H. de Oliveira, R. de Araujo, A. Loureiro,  
909 Drina: a lightweight and reliable routing approach for in-network aggregation  
910 in wireless sensor networks, *IEEE Trans. Comput.* 62 (4) (2013) 676–689.
- 911 [24] Y. Jin, S. Gormus, P. Kulkarni, M. Sooriyabandara, Link quality aware and con-  
912 tent centric data aggregation in lossy wireless networks, in: Proceedings of  
913 the 2014 IEEE Wireless Communications and Networking Conference (WCNC),  
914 2014, pp. 3082–3087.
- 915 [25] S. Madden, M.J. Franklin, J.M. Hellerstein, W. Hong, Tag: a tiny aggregation  
916 service for ad-hoc sensor networks, *SIGOPS Oper. Syst. Rev.* 36 (SI) (2002)  
917 131–146, doi:10.1145/844128.844142. URL <http://doi.acm.org/10.1145/844128.844142>.
- 918 [26] S. Motegi, K. Yoshihara, H. Horiuchi, Dag based in-network aggregation for sen-  
919 sor network monitoring, in: Proceedings of the International Symposium on  
920 Applications on Internet (SAINT '06), IEEE Computer Society, Washington, DC,  
921 USA, 2006, pp. 292–299, doi:10.1109/SAINT.2006.20. URL <http://dx.doi.org/10.1109/SAINT.2006.20>.
- 922 [27] Y. Wu, Z. Mao, S. Fahmy, N. Shroff, Constructing maximum-lifetime data-  
923 gathering forests in sensor networks, *IEEE/ACM Trans. Netw.* 18 (5) (2010)  
924 1571–1584, doi:10.1109/TNET.2010.2045896.
- 925 [28] A. Sharaf, J. Beaver, A. Labrinidis, K. Chrysanthis, Balancing energy efficiency  
926 and quality of aggregate data in sensor networks, *VLDB J.* 13 (4) (2004) 384–  
927 403, doi:10.1007/s00778-004-0138-0.
- 928 [29] I. Solis, K. Obraczka, The impact of timing in data aggregation for sensor net-  
929 works, in: Proceedings of the 2004 IEEE International Conference on Commu-  
930 nications, 6, 2004, pp. 3640–3645 Vol.6, doi:10.1109/ICC.2004.1313222.
- 931 [30] D.S.J. De Couto, D. Aguayo, J. Bicket, R. Morris, A high-throughput path metric  
932 for multi-hop wireless routing, in: Proceedings of the 9th Annual International  
933 Conference on Mobile Computing and Networking (MobiCom '03), ACM, New  
934 York, NY, USA, 2003, pp. 134–146.
- 935 [31] N. Tsiftes, A. Dunkels, A database in every sensor, in: Proceedings of the 9th  
936 ACM Conference on Embedded Networked Sensor Systems (SenSys '11), ACM,  
937 New York, NY, USA, 2011, pp. 316–332, doi:10.1145/2070942.2070974.
- 938 [32] S. Nath, Energy efficient sensor data logging with amnesic flash storage, in:  
939 Proceedings of the 2009 International Conference on Information Processing  
940 in Sensor Networks (IPSN '09), IEEE Computer Society, Washington, DC, USA,  
941 2009, pp. 157–168.
- 942  
943

UNCORRECTED

FREE  
paper  
مقاله  
رایگان